Steering product formation in high-pressure anaerobic digestion systems:

The effect of elevated CO_2 partial pressure in the degradation of glucose and glycerol by a mixed culture

MSc. Thesis

Yu-ting (Kelly) Chang

December 2019

TU Delft

Steering product formation in high-pressure anaerobic digestion systems:

The effect of elevated CO_2 partial pressure in the degradation of glucose and glycerol by a mixed culture

---

The thesis is submitted to Delft University of Technology in partial fulfillment of the requirements for the degree of

Master of Science in Civil Engineering,
Environmental Engineering Track

By Yu-ting Chang
9th December 2019

Graduation committee:

Prof. dr. ir. J.B. van Lier
Delft University of Technology
Faculty of Civil Engineering and Geosciences
Department Sanitary Engineering

Dr. ir. R.E.F. Lindeboom
Delft University of Technology
Faculty of Civil Engineering and Geosciences
Department Sanitary Engineering

Dr. L. Jourdin
Delft University of Technology
Faculty of Applied Sciences
Department of Biotechnology, Bioprocess Engineering section

Ir. Pamela Cerón Chafla
Delft University of Technology
Faculty of Civil Engineering and Geosciences
Department Sanitary Engineering

Preface

The unforgettable journey in TU delft will be ended along with the thesis work comes to the final stage. Obtaining the Master degree is not an easily accomplished task for me, but I am truly grateful to all the ups and downs I experienced during the thesis that urged me to be stranger and learn how to deal with problems better in the future. At the same time, I am feeling gratitude for all the support throughout the process.

This thesis work would have been impossible to finish without the help of lots of people in the past 10 months. First, I would like to express my gratitude to my graduation committee Prof. Jules van Lier, Assistant Professor Ralph Lindeboom, Assistant Professor Ludovic Jourdin, and Ir. Pamela Cerón Chafla for giving me valuable suggestions and constructive feedback to make the outcome more comprehensive. I highly appreciate them sharing their knowledge and passion for anaerobic digestion as this has truly inspired me to generate more satisfactory results.

I am also grateful to the PHDs working in the red lab, especially Victor, lab technician, Armand, and Lais for helping me during the experimental period in the laboratory by offering me the required resources.

I was also lucky to have many accompanies during this stressful period. Thank you, my Taiwanese friends, Flora, Rose, Lun, Lawrance, Chao, Kao, and Shinny for taking care of me when I was drained out. Thank you, Tavishi, for being the best person to talk to, and introducing me to your interesting Indian friends who lit up my dull life. Thank you, my boyfriend, Sean, for always being there with me to share all the tears and laughter. Thank you, Vincent and Kelly, my training buddies, for encouraging me to stay healthy. Thank you, Dispuut 63 and 64, for always giving me warm greeting whenever I come by the Dispuut. Thank you, Magnolia, Daniel, Beatriz, Lais, Victor, HongXiao, and all my friends working in the red lab, for accompanying me the 6 months of lab life. Thank you, GVR group, for offering each other mental support when necessary.

Finally, I would like to deeply acknowledge my parents for their unconditional love during this study and my life. They always have my back and make me brave enough to pursue my dream. Thank you, I love you!

Abstract

Biogas is the well-known product of Anaerobic Digestion (AD), but nowadays, the intermediate products (volatile fatty acids - VFAs) of anaerobic metabolism have gained increasing attention inside the “carboxylate platform”. However, steering and optimizing the process for selective metabolite production is still an unraveled task inside this field since it relies on the manipulation of operational parameters. The objective is to understand the conversion of glucose and glycerol in the mixed culture of anaerobic digestion to unravel possibilities to steer product formation.

Glucose and glycerol are the main components in the waste streams of beverage and biodiesel industries. Regarding the degradation pathways in AD, both glucose and glycerol are oxidized to pyruvate by fermentative bacteria to obtain energy and metabolic intermediates under anaerobic conditions through the same intermediate, glyceraldehyde-3-phosphate. Pyruvate, the key branching-point, allows the process to enter different metabolic pathways which lead to the formation of various metabolites. Under the fermentation conditions, redox balance is necessary to be maintained through terminal electron transfer to internally produced compounds. Since glycerol has a higher degree of reduction than glucose (Glucose: 0.33 NADH/C-Glucose; Glycerol: 0.66 NADH/C-Glycerol), the conversion of glycerol into pyruvate generates a double amount of reducing equivalents. On the one hand, this provides the advantage of higher theoretical product yield of reduced compounds. On the other hand, half of the glucose is lost as CO_2 during the fermentation, and this reduces the product yield.[1] Therefore, we assume that elevated pCO_2 could have a more significant detrimental effect on glucose fermentation.

In this research, batch experiments at different pCO_2 (0.3, 1, 3, 5, 8 bar) were performed, and different types of measurements and analyses were employed to monitor the pCO_2 effect on the metabolism. We designed some of the potential pathways of glucose and glycerol conversion under elevated pCO_2. The elevated pCO_2 converged the product spectrum of both substrates towards propionate production but affected the degradation and production phase of propionate and acetate. Initial pCO_2 of 0.3 bar and 1 bar did not cause visible inhibition on the propionate production of both substrates. However, the propionate degradation was kinetically affected under 0.3 and 1 bar initial pCO_2. Although propionate was degradable, its degradation phase at 1 bar initial pCO_2 was longer than 0.3 bar. On the contrary, when the pCO_2 was elevated to 3, 5, and 8 bar, not only the propionate production phase became longer, but also the

maximum concentration became lower on both substrates. Moreover, propionate degradation was ceased. The lower propionate production was suspected to be due to the inhibition of NADH production as a consequence of the elevated pCO_2 effect. The undegradable propionate might be attributed to unfavored decarboxylation reactions under elevated pCO_2.

The enrichment approach was applied to examine the adaptability of the microbial consortium under the CO_2-exposing environment. Therefore, not only the more predominant metabolic reaction would be favored during the enrichment, but also changes in the community due to CO_2 influence were expected. Propionate degradation was achieved with this inoculum at the only tested condition (5 bar initial pCO_2). From the community analysis, *Smithella* was enriched during the enriched and it was suspected to play a significant role in the propionate conversion.

Besides, the difference between the substrates on the fermentation has been observed. Due to the higher available reducing power of glycerol than glucose, glycerol was potentially able to generate more propionate. However, the butyrate formation also needs the reducing power to proceed with the reaction, but it was not detected in the glycerol fermentation. Therefore, reducing power distribution from specific substrates with elevated pCO_2 might also be affected. Moreover, the substrate was also hypothesized to influence cell viability, where glycerol fermentation increased the cell viability but glucose not. The degradation of acetate and butyrate in the non-enriched inoculum was observed to be kinetically affected by elevated pCO_2, with the later becoming undegradable at 8 bar. The reason for this phenomenon needs further investigation.

Table of Content

List of Figures

List of Tables

1. Introduction

1.1. Problem definition

Conventional Anaerobic Digestion (AD) is widely applied to treat activated sludge, where microorganisms consume organic pollutants. AD used to be considered as a treatment process to produce biogas, and it has now gained more attention because it is considered as one of the “green” solutions to combat climate change due to its distinct advantage. AD not only performs sludge treatment but also acts as a biorefinery platform.

In the AD process (Fig. 1), VFAs can be accumulated at the stage of acidogenesis and acetogenesis if the inhibition of methanogenesis occurs[2]. These bio-based VFAs can be recovered and utilized in chemical industries. Although various fermentation processes have been developed, they have not yet been widely applied in the industry due to the low selectivity and yields. VFAs production through AD could result in low output value without a proper steer. High purity of the acid-containing stream reduces the recovery effort and generates higher output value. Minimizing the product spectrum is undoubtedly beneficial, whereas bio-augmentation and recovery methods are required for further research to enable sustainable and economic-feasible production.[3]

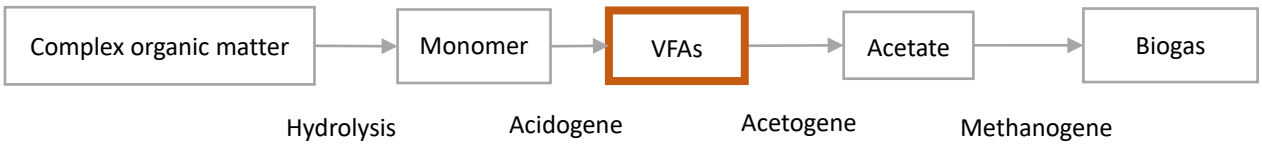

Figure 1. Overall scheme of AD process

If biogas is still the targeted end-product of AD, the optimization of the CH_4 content is of interest. Several alternatives have been proposed to upgrade biogas, and among them, the process of autogenerative high-pressure anaerobic digestion has been proposed. Autogenerative high-pressure anaerobic digestion is a technique that accumulates the generated biogas in the system to enhance the pressure and further improve the biogas quality. As a working principle, it improves the quality because more CO_2 remains dissolved than methane in the water phase due to the difference in gas solubility at elevated biogas pressure. However, the dissolved CO_2 appeared to cause and increasing level of VFA in the liquid broth[4].

Even though CH_4 production provides AD an advantage over other environmental

technologies, where waste is converted into energy during water treatment, the production of VFAs and/ or alcohol instead of biogas from AD has also been recognized as a new approach to applying this resource recovery platform over recent years.[5] The concept of biorefinery from International Energy Agency (IEA): “Biorefining is the sustainable processing of biomass into a spectrum of marketable products and energy.”[6] Biogas production is a well-known biorefinery platform of AD where the biomass is converted into biogas due to a series of biochemical reactions carried out by bacteria and archaea[7]. Additionally, AD could potentially become part of the “carboxylate platform” to produce volatile fatty acids (VFAs) during microbial metabolism[8]. This platform deals with the process of converting organic feedstock into short-chain carboxylates as intermediate feedstock chemicals[8]. The biorefinery concept of VFAs recovery could be appealing to chemical industries since the waste streams will not be wasted but treated as raw materials instead.

VFAs production relies on the tuning of operational parameters to trigger metabolic responses to stress conditions. Therefore, the operation conditions play a significant role in the selective process since they influence AD processes fundamentally. The operational parameters, such as pH, substrate concentration[9], temperature[10], salinity[11,12], headspace composition[13,14], could all be the factors that steer end-product formation in mixed culture fermentation.[15] However, this research focused on the effect of headspace composition, especially elevated pCO_2, to the selectivity of the degradation pathway. Nevertheless, the product recovery is as crucial as the fermentation processes optimization, and it is often the most challenging part of the entire process.[16] The recovery of a single compound is more valuable but difficult; therefore, efforts shall be made to have a selective production that facilitates downstream processing. This stress factor could also become a selecting factor, where the dissolved CO_2 could affect microbial activity in the anaerobic bioreactor and steering the product formation additionally.

The project, “Steering Product Formation in High-Pressure Anaerobic Systems”, has been on-going since 2016. The main objective is to understand the effect of elevated CO_2 partial pressure (pCO_2) on the metabolic pathways of the conversion of complex substrates in mixed culture to elucidate the effect of pCO2 on the pathway feasibility and to unravel possibilities to steer product formation. The undefined nature of the microbial community in the anaerobic reactor is the main factor that complicates the steering process, where the interactions among microorganisms are rather complex. Investigation of microbial interspecies interactions is essential for elucidating the function of microbial systems and steer the product formation with specific operational

conditions. The yield capacity and efficiency could also be enhanced with a better understanding of microbial metabolism in the system, which allows us to increase the selectivity of end-product formation and obtain economically-attractive end-products.

Previously, the project had selected the experimenting inoculum, the experimental set-up of batch reactors, and reactor operation. Moreover, the conversion of simple substrates, including acetate, propionate, butyrate, pyruvate had been investigated since the reasoning behind the project is to apply a bottom-up approach to understand the conversion of real complex substrates. The conversion of defined simple substrates such as acetate was clarified by other researchers at first, where the substrates have a closer connection with biogas production, then the project moved on to the more complex substrates. Regarding the previous experimental results, they had been established that increasing pCO_2 in the anaerobic bioreactor decreases the degradability of propionate and the conversion rate of butyrate to acetate. Also, the main metabolite from pyruvate was found to be propionate with increasing pCO_2. Currently, the investigation on the degradation of more complex substrates than before was proceeded by this study.

This thesis focuses on the conversion of glucose and glycerol in AD under elevated pCO2, and both are just one step above pyruvate via glycolysis. The reason why they are worth researching is, on the one hand, that in the wastewater of food and beverage industries, a large amount of sugar remains as residue, and glucose is the primary end-product of the hydrolysis of polysaccharides. On the other hand, the production of biodiesel has increased due to strategies for securing energy resources, because of it, approximately 100 g of glycerol is generated as a byproduct for each kilogram of biodiesel that is produced.[17,18] Batch experiments were conducted to study the effect on the conversion of these substrates and the microbial response triggered by elevated pCO_2. An enrichment approach was applied to examine the adaptability of the microbial consortium under the CO_2-exposing environment. Therefore, not only the more predominant metabolic reaction would be favored during the enrichment, but also changes in the community due to CO_2 influence were expected. Liquid and gas samples were taken to understand the hypothetical pathways by observing the concentration changes. On the other hand, the dynamics of microbial communities were analyzed to get a more in-depth insight into the CO_2 effect.

1.2. Research question

Main research question 1:

Are there significant differences in the conversion 1 g COD/L (glucose/glycerol) substrate under conditions of elevated CO_2 while using enriched and non-enriched anaerobic inocula extracted from the same reactor?

Sub-research questions:

- What is the effect of elevated pCO_2 on the production of the three main intermediate metabolites (i.e., propionate, butyrate, acetate) in both cultures?
- What is the effect of elevated pCO_2 on the methane production in both cultures?

Main research question 2:

Are there observed effects on the cell viability and the community structure under elevated pCO_2 in both enrichment culture and non-enrichment culture by using 1 g COD/L (glucose/glycerol) substrate?

2. Literature review

2.1. Anaerobic degradation of complex organic compounds

Anaerobic digestion (AD) is a process where a series of microbial conversions mediated by functionally and phylogenetically diverse bacteria and archaea occurs. These microorganisms are mainly fermentative, acetogenic and methanogenic[19,20]. However, if there is the presence of polymeric organic compounds (e.g., polysaccharides, lipids, proteins), hydrolysis will be the first step. (Fig. 1) Since the polymeric organic compounds cannot enter the microorganism, the microorganism, including the representatives of the Firmicutes (Clostridia, Bacilli), Bacteroidetes and Gammaproteobacteria[21], excrete extracellular enzymes to catalyze the cleavage of ester bonds, glycoside bonds, and peptide bonds[21]. The fermentative bacteria function in the acidogenesis stage where the conversion of monomers into intermediate products such as propionate, butyrate occurs. Acetogens convert the intermediate products to acetate and release hydrogen, then acetate consumption by the methanogen is carried out. Instead of this consecutive reaction for anaerobic degradation, acetogens and methanogens can also exploit different pathways for acetate and methane production.

Acetogenesis can be derived from two routes; first, the conversion of intermediate products of acidogenesis, including carbohydrates, organic acids, and alcohols, into acetate, and second, the reduction of CO_2 by H_2, known as homoacetogenensis. Homoacetogenesis happens via the Wood-Ljungdahl pathway (WLP), where two molecules of CO_2 are reduced to acetate by hydrogen with acetyl-CoA as intermediate[22] (Eq.1). Schuchmann stated that all acetogens examined to date contain the WLP, and all enzymes of the WLP are soluble cytoplasmic enzymes[23]. Nevertheless, it is also essential to notice that some acetogens produce no acetate as end product[24]; therefore, acetyl-CoA should also be defined as a product from two molecules of CO_2 shared by all acetogens.

The acetogenesis stage of AD is equally vital because it reflects the efficiency of biogas production. The major substrates consumed by methanogens are acetic acid (CH_3COOH), methanoic acid ($HCOOH$), carbon dioxide (CO_2), dimethylsulfate ($(CH_3)_2SO_4$)), methanol (CH_3OH), and methylamine (CH_3NH_2)[25], where approximately 70% of CH_4 is formed through acetoclastic methanogenesis[26] (Eq. 2). While hydrogenotrophic methanogenesis is another pathway of biogas generation, where one mole CO_2 is reduced by hydrogen and form methane[27] (Eq. 3). The three

equations can actually form a loop as Fig. 2, and the hydrogen pressure determines the direction of acetogens; under low hydrogen pressure in a well-balanced fermentation, the acetogens tend to go left; otherwise, it goes to the right[23]. Besides, the hydrogen pressure can also be affected by acidogenesis, which generates part of hydrogen.

$$2CO_2 + 4H_2 \leftrightarrow CH_3COO^- + H^+ + 2H_2O \ \ \Delta G^{0\prime} = -95kJ/mol \quad \text{(Eq. 1)}$$

$$CH_3COO^- + H^+ \leftrightarrow CH_4 + 2CO_2 \ \ \Delta G^{0\prime} = -36kJ/mol \quad \text{(Eq. 2)}$$

$$CO_2 + 4H_2 \leftrightarrow CH_4 + 2H_2O \ \ \Delta G^{0\prime} = -131kJ/mol \quad \text{(Eq. 3)}$$

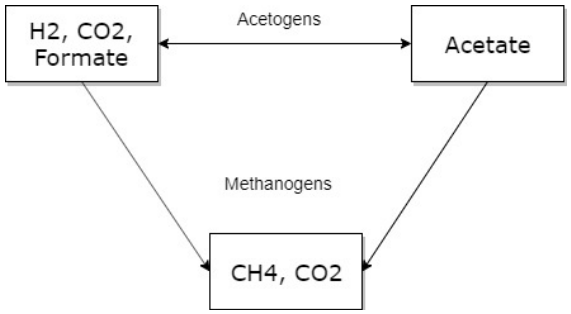

Figure 2. The interaction between acetogens and methanogens

2.2. The energetic barrier in AD

Reaction energetics challenge the AD processes due to the small amount of free energy in the methanogenic degradation of complex organic compounds. Under standard conditions, the oxidation of butyrate, propionate, and other non-gaseous products of acidogenesis is endergonic; however, when the oxidation processes are coupled to hydrogenotrophic methanogenesis, the conversion becomes energetically feasible.[28] The small amounts of free energy have to be exploited efficiently by bacteria and archaea living syntrophically.

Syntrophic cooperation processes rely on an interspecies electron transfer (hydrogen/formate). The syntrophic mechanism supports the conversion of VFAs (e.g., propionate oxidation) into acetate, CO_2, and H_2[28–31], where hydrogenotrophic methanogens act as hydrogen-scavenging archaea to maintain the pH_2 sufficiently low [29,32,33]. For example, the propionate oxidation should work syntrophically with hydrogenotrophic methanogenesis to maintain both reactions thermodynamically feasible ($\Delta G^{0'} < 0$ kJ/mol). In Fig. 3, the blue regions represented the feasible syntrophic reactions of propionate oxidation and hydrogenotrophic methanogenesis under different pH_2. The acetogens can be inhibited when the pH_2 exceeds 10^{-4} atm[34]. The pH_2 would become too high to have the propionate oxidation thermodynamically infeasible ($\Delta G^{0'} > 0$ kJ/mol) if the transfer is not well-functioned between syntrophic

propionate-oxidizing bacteria and hydrogenotrophic methanogen. Therefore, when the feasibility of the hydrogen transfer is affected, it could further cause an influence on the metabolites. The metabolic abilities of syntrophic partners not only overcome the energetic barriers but further metabolize intermediates that can hardly be degraded by a single cell[35]. Nevertheless, the region of feasible reactions can be changed by different pCO_2 conditions. (Fig. 3A and Fig. 3B)

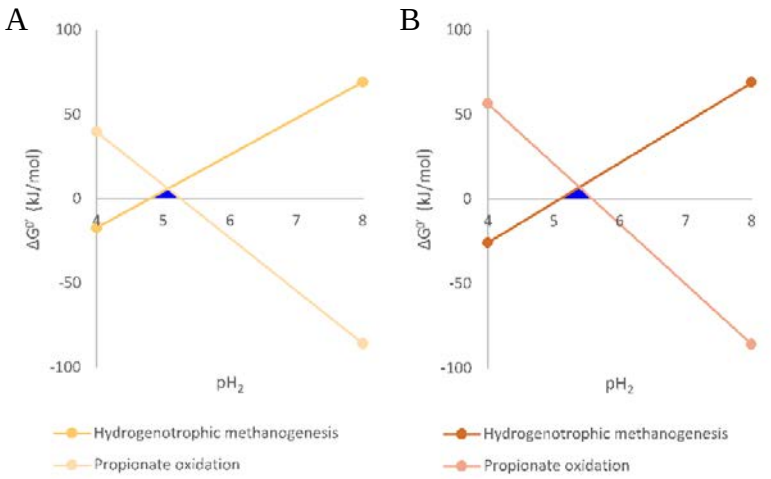

Figure 3. The relationship between propionate oxidation and hydrogenotrophic methanogenesis with different pH_2 (4-8 bar) under the initial pCO_2 of 0.3 bar (Fig. 3A) and 8 bar (Fig. 3B) with the temperature of 35°C, pH of 7.37 (3A)/ 5.94 (3B), and [propionate], [water], [methane] = 1 M (bar).

2.3. High-pressure anaerobic degradation of complex organic compounds

Autogenerative high-pressure digestion (AHPD) was developed for biogas upgrading; the technology accumulates the biogas generated through anaerobic digestion processes to create high pressure in the headspace. Meanwhile, methane and CO2 possess different physical properties of liquid and gas, where CO2 has a higher solubility than methane. Therefore, the high pressure makes the CO_2 dissolves in the liquid phase more than methane to enhance biogas quality. Lindeboom *et.al* proposed that anaerobic microorganisms originating from non-pressurized digesters enabled autogenerate biogas pressure up to 90 bar[36]. No significant influence has been observed on the degradation of the organics and biogas production when the initial pressure is under 30 bar[37], and thus, the mere pressure effect was not able to affect the metabolism.

However, the accumulation of CO_2 in either water or headspace was seen to affect microbial metabolism. Kato *et al.* found that high concentrations of CO_2 (113.4 mmol/L) suppressed more than 50% of methanogenic rate on the syntrophic co-culture of

Methanothermobacter thermautotrophicus and *Thermacetogenium phaeum*, but it barely affected the methanogenic rate of pure acetoclastic methanogen culture, *Methanosaeta thermophila*.[38] Lindeboom *et al.* demonstrated that the specific propionate oxidation rate of the CO_2-adapted consortium decreased linearly from 45.8 to 3.3 mg COD g VS^{-1} day^{-1} with increasing pCO_2 from 1 bar to 5 bar, where 90% of the degradation was inhibited[39]. Nevertheless, more fundamental research is needed to investigate the influence of elevated pCO_2 on the anaerobic conversion of different substrates. Arslan *et.al* explained the potential effect of headspace composition on the selectivity of a metabolic pathway in AD. Carboxylate concentrations and fractions could be directed by supplying different ratios of hydrogen and carbon dioxide in the headspace in mixed culture fermentation, where selective butyrate production reaching 75% fraction was found under the 2 bar pCO_2 headspace on carbohydrate-rich waste.[13]

According to Henry's law, the solubility of a certain gas is proportional to the partial pressure of the gas. ($k_{H,\ 35°C}$ of CO_2: 0.0012 mol/L bar). Due to the high pCO_2 supplementation in the headspace, the pH can be decreased from the CO_2 dissolution. As CO_2 dissolves in the water, H^+ and HCO_3^- are produced from H_2CO_3 ionization (Eq. 4); therefore, the pH decreases from the proton liberation.

$$CO_2 + H_2O \leftrightarrow H_2CO_3 \leftrightarrow H^+ + HCO_3^- \qquad \text{(Eq. 4)}$$

Methanogens were reported to be more active in the pH range of 6.5-8[40]. Acetoclastic bacteria can also be inhibited by increasing acidity[19], resulting in an accumulation of propionate and butyrate proportional to the decreasing pH of the solution[41]; however, high VFA concentrations cause pH values to decrease and result in toxic conditions in the reactor. Murto *et al.* proposed that when the system is highly buffered VFAs concentration will be the only reliable parameter for process monitoring.[42] On the other hand, various VFAs existing in ADs have different and cooperative effects on bacteria and archaea. Wang *et al.* reported that the propionate concentration of 900 mg/L resulted in serious inhibition of the methanogenesis, while the acetate and butyrate concentrations of 2400 and 1800 mg/L, respectively, resulting in negligible inhibition of the methanogenesis.[43] on the other hand, Ingrid's findings showed that the microbial communities were able to withstand variation in VFA concentrations when the AD systems had the good buffering capacity.[44] Since this research focuses on the effect of CO_2 itself on metabolism, the effect of pH variation and VFA variation on the experiments should be minimized. Sodium bicarbonate (100mM) was chosen as a buffer to keep as much as CO_2 effect during the buffering.

CO_2 is regarded as both an intermediate and end-product in AD since methanogens can either consume CO_2 and methane or exploit hydrogen as the electron donor to drive the CO_2 reduction into methane.[9] Although CO_2 was reported having a positive impact on the anaerobic growth of *E. Coli* and the biosynthesis of small molecules, fatty acids, central metabolites from glycerol under acidic conditions[1]. CO_2 has been also considered inhibitory/toxic to microbial metabolism, particularly for cell growth and yeast fermentation[45]. There were different hypotheses and finding on the CO_2 toxicity. Hansson et al. assumed that CO_2 dissolution in cell membranes would increase membrane fluidity and impair its function[10]. The increase of CO_2 concentration from 0 to 30000 ppm was also found to make the membrane electrical potential decrease, causing a decrease in proton motive force[46]. Sufficient proton motive force allows the proton to be transferred into the matrix, and this directly affects ATP synthesis. The reaction of converting ADP into ATP requires a proton transporting through a symporter, and thus, the proton potential between matrix and the intermembrane space is essential.

2.4. Fermentation processes of glucose versus glycerol

Regarding the degradation pathway in AD, both glucose and glycerol are oxidized to pyruvate through the same glycolysis intermediate, glyceraldehyde-3-phosphate, by fermentative bacteria to obtain energy and metabolic intermediates under anaerobic conditions[47,48] (Fig. 4, red lines). Pyruvate, the key branching-point, allows the process to enter several different metabolic pathways, and lead to the formation of various metabolites. Under the fermentation conditions, redox balance is necessary to be maintained through terminal electron transfer to internally produced compounds. Since glycerol has a higher degree of reduction than glucose (Glucose: 0.33 NADH/C-Glucose; Glycerol: 0.66 NADH/C-Glycerol), the conversion of glycerol into pyruvate generates a double amount of the reducing equivalents[49]. On the one hand, this provides the advantage of higher theoretical product yield of reduced compounds. On the other hand, half of the glucose is lost as CO_2 during the fermentation, and this reduces the product yield.[1] Therefore, we assume that elevated pCO_2 could have a more significant detrimental effect on glucose fermentation.

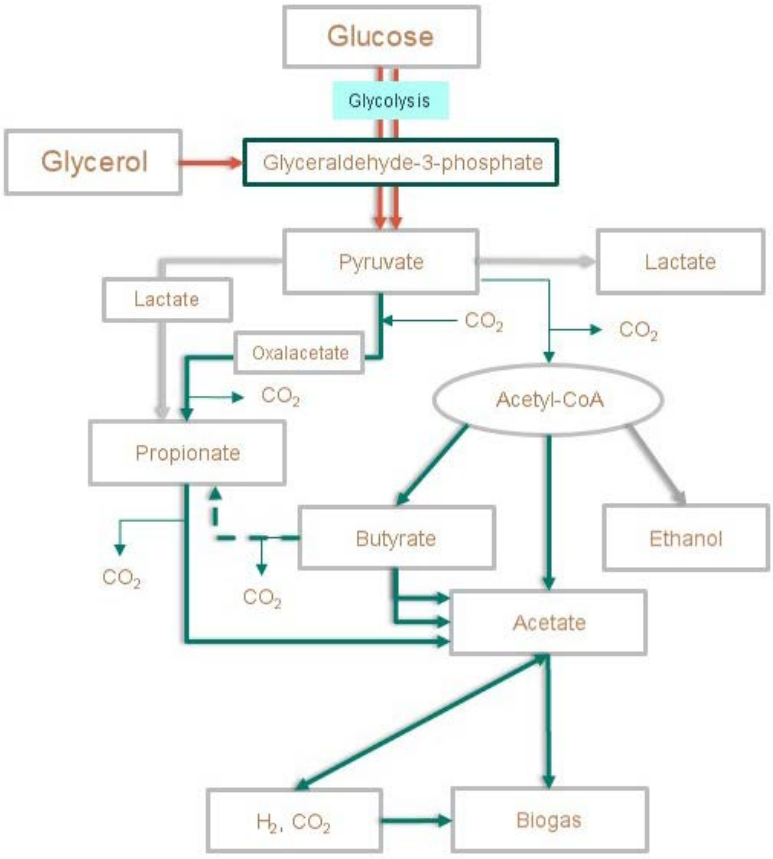

Figure 4. Metabolic pathways of the fermentation of glucose and glycerol (Redline: pathway of glucose/ glycerol to pyruvate, adapted from the literature[50]; green line: the observed pathways of the intermediate compounds from previous study in the project, adapted from the thesis[51]; gray line: the intermediate products were not observed in the pathways of the researched compounds)

The produced metabolites, propionate, ethanol, butyrate, and acetate can be further utilized by the microbial consortium. The predominant metabolism is controlled by prevailing biological, environmental, thermodynamic conditions of the system.[8] According to previous work inside this project, the promoted catabolic pathway in pyruvate conversion under elevated pCO_2 was towards propionate[51] (Fig. 5), since the excess CO_2 might favor the carboxylation reaction from pyruvate to succinate. The undegradable propionate might be attributed to the excessively available CO_2 that could have caused an impact on the enzymatic activity, for example, in propionate CoA-transferase, a key enzyme catalyzing the conversion of propionate into acetate. Furthermore, pyruvate was found to degrade towards propionate and acetate selectively. It was hypothesized that ATP and reducing power were probably synthesized from the pyruvate oxidation to acetate, and further benefited the propionate production pathway.[51]

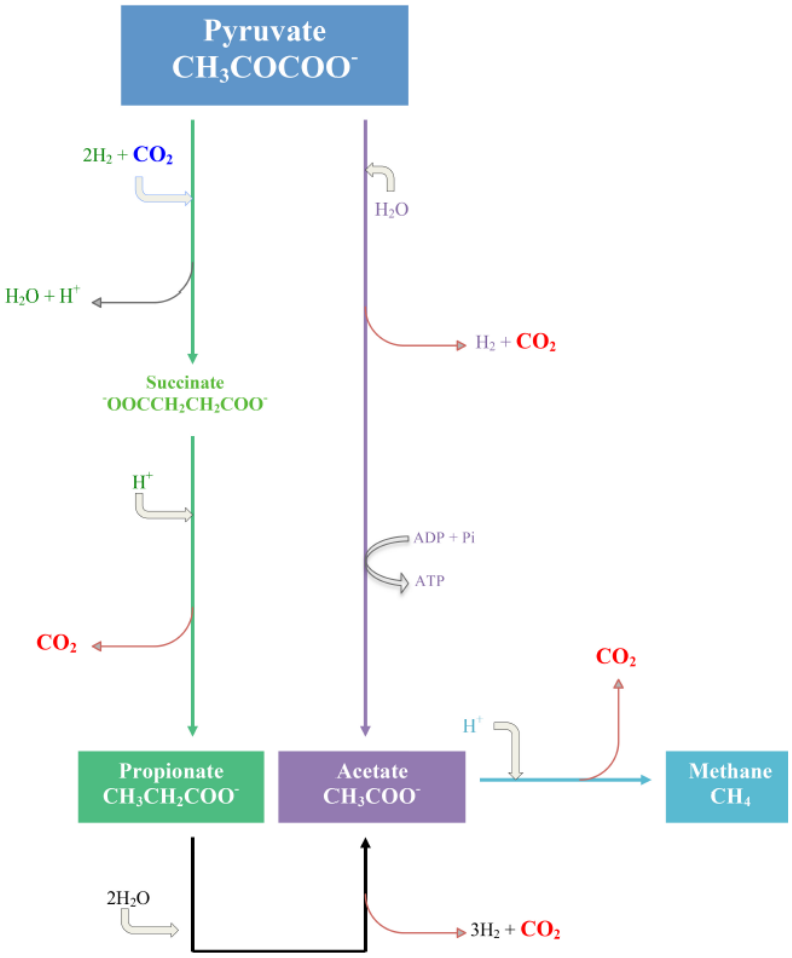

Figure 5. Major catabolic pathways involved in the anaerobic degradation of pyruvate at different pCO_2[51]

Besides the propionate production from pyruvate, it can produce from butyrate degradation as well. However, in the previous study by Gomez Paez[51], the butyrate was prone to produce acetate instead of propionate with the elevated pCO_2.

2.5. Propionate-producing pathways

Under the tested experimental conditions, propionate can be possibly produced via several metabolic pathways, which can be classified into two major groups: fermentative and biosynthesis pathways (Fig. 6A, 5C).

2.5.1. Fermentative pathways

Propionate, a primary fermentation product, can be produced through the acryloyl-CoA pathway, the 1,2-propanediol pathway, the methylmalonyl-CoA or succinate pathways

(Table 1). Compared to biosynthesis pathways, fermentative pathways provide energy and help consume reduced cofactors that result from the catabolism of sugars.[52] Both their role in energy generation and maintaining a redox balance permit these pathways to be coupled to growth[52].

Among these pathways, only the succinate pathway is more plausible to occur with elevated pCO_2 due to the ability of CO_2 incorporation. Although an ATP is consumed to convert CO_2 and pyruvate/ phosphoenolpyruvate into oxaloacetate, this is at least partially compensated by an anaerobic electron transport chain consisting of the NADH dehydrogenase and fumarate reductase[52].

2.5.2. Biosynthesis pathways

The 3-hydroxypropanoate (3HP) and 4-hydroxybutanoate (4HB) cycles are also possible to be carried out due to their capacity to fix CO_2 as sole carbon source. These pathways associated with anabolic metabolism lead to the synthesis of propionyl-CoA[52]. Both cycles enable carbon fixation for biomass generation through an acetyl-CoA/propionyl-CoA carboxylase[53] and only differ in the final steps, where the 3HP cycle fixes carbon dioxide to glyoxylate, whereas the 4HB cycle generates acetyl-CoA. However, the high ATP requirements is the major constrain of these pathways; the reactions consume a net two ATP and two NADPH per acetyl-CoA consumed, resulting in a maximum theoretical yield of 1.33 mol propionate/mol glucose with no ATP generation.[52]

Table 1. Microbial species able to generate propionic acid during fermentation[52]

Microorganism	Substrates	Products	Pathway
Propionibacteria acidipropionici *P. freudenreichii* [1] *P. shermanii* [2]	Glucose, sucrose, lactate, glycerol	Propionate, acetate, succinate, CO_2	Wood-Werkman cycle (Figure 1(AIII))
Clostridia propionicum	Glycerol, lactate, alanine, serine, threonine	Propionate, succinate, formate, acetate, n-propanol	Acrylate pathway (Figure 1(AII))
Bacteroides fragilis B. ruminicola	Glucose	Acetate, lactate propionate, succinate, formate, CO_2	Succinate pathway (Figure 1(AIV))
Veillonella parvula V. alcalescens	Lactate, succinate	Propionate, acetate, CO_2, H_2	Succinate pathway (Figure 1(AIV))
Propionigenum modestum	Succinate	Propionate, CO_2	Succinate pathway (Figure 1(AIV))
Selenomonas ruminantium *S. sputigena*	Lactate Glucose	Propionate, lactate, acetate, CO_2	Succinate pathway (Figure 1(AIV))
Megasphaera elsdenii	Lactate	Acetate, propionate, butyrate	Acrylate pathway (Figure 1(AII))
Salmonella typhimurium	Deoxy sugars, glucose, 1,2-propanediol	1,2-propanediol, propanol, propionate, acetate, formate, lactate, CO_2	1,2-propanediol pathway (Figure 1(AI))

[1] *P. freudenreichii subsp. Freudenreichii;* [2] *P. freudenreichii subsp. Shermanii.*

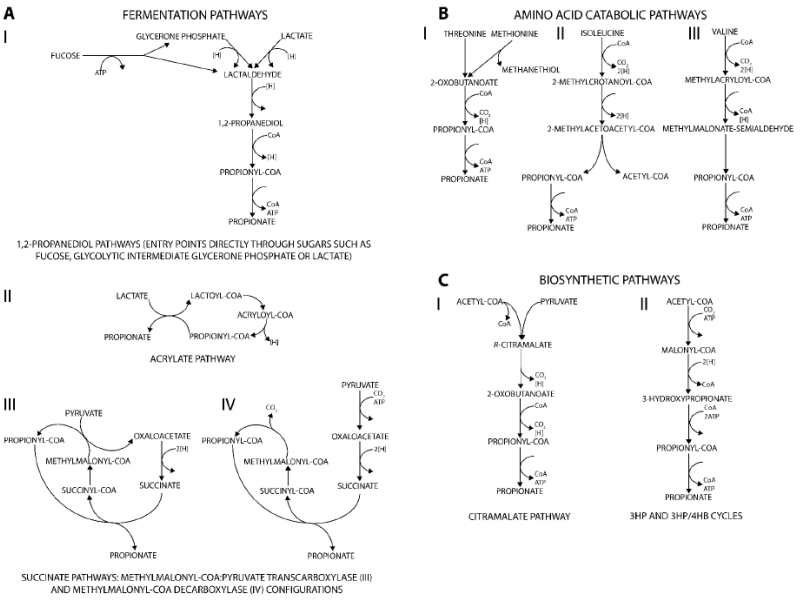

Figure 6. The biological propionate-producing pathways[52]

3. Methodology

3.1. Experimental design

This thesis focused on the effect of elevated pCO_2 on the degradation of two specific substrates, namely glucose and glycerol. As seen Exp. 1 and Exp. 2 in Fig.7, the anaerobic conversion of each substrate was carried out using non-enriched and enriched inoculum. The non-enriched-inoculum fermentation was incubated in batch under 5 different initial pCO_2: 0.3, 1, 3, 5, 8 bar and the enriched inoculum was incubated with the initial pCO_2 of 5 bar since the pCO_2 is the condition started causing the clear difference among the experimental conditions.

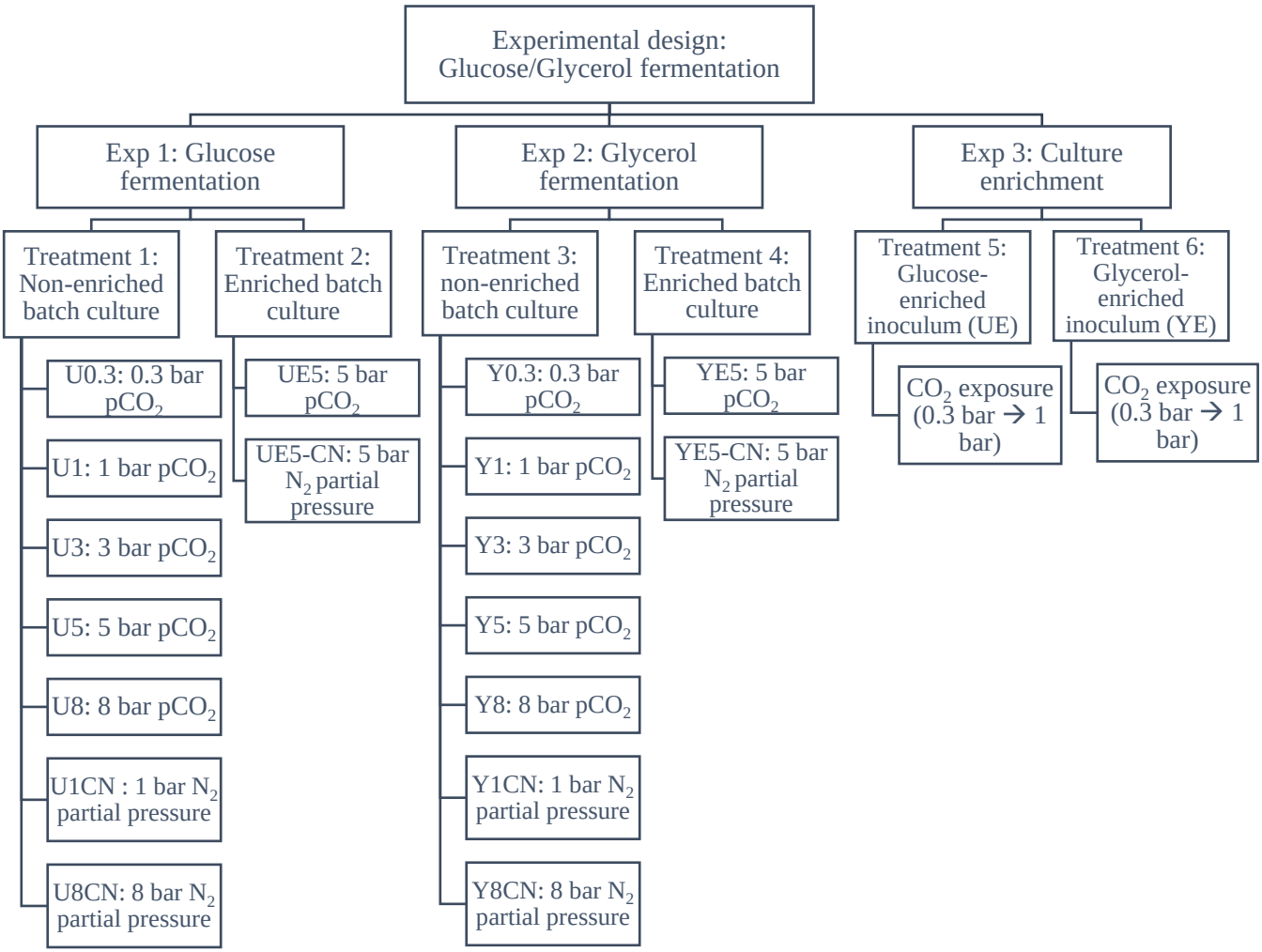

Figure 7. Overall experimental design

3.2. Inoculum

3.2.1. Non-enriched inoculum (NEI) characteristics

Flocculent anaerobic sludge obtained from an AnMBR plant treating food industry wastewater was used as starting inoculum. Due to the complexity of the microbial consortium and chemical composition, sludge characterization is a preliminary identification, which facilitates the understanding of the sludge properties. The sludge characterization has been defined by the previous research[51] and is shown in Table 2.

Table 2. Physio-chemical characterization of the non-enriched inoculum

Parameter	**Unit**	**Mean**	**STD**
TCOD	g/L	22.22	0.52
SCOD	g/L	1.92	0.04
TOC	g/L	7.72	0.83
TSS	g/L	15.87	0.07
VSS	g/L	13.62	0.06
VSS/TSS	%	85.80	0.09
NH_4-N	mg/L	107	2
TP	mg/L	112	0.9
pH	-	7.3	-

3.2.2. Enriched inoculum characteristics

The non-enriched inoculum was enriched with two substrates, respectively. After the enrichment, the inoculum was centrifuged and resuspended with the fresh medium, including the micronutrient, macronutrient and buffer instead of the substrate. The processed enriched inoculum characterization is presented in Table 3.

Table 3. Physio-chemical characterization of the enriched inoculum

Parameter	Unit	Mean	STD	Mean	STD
		Glucose-enriched inoculum		Glycerol-enriched inoculum	
TCOD	g/L	3.54	0.55	6.78	0.06
SCOD	g/L	0.070	0.005	0.162	0.004
TOC	g/L	0.680	0.006	0.704	0.003
TSS	g/L	3.54	0.09	6.03	0.08
VSS	g/L	2.86	0.03	4.93	0.01
VSS/TSS	%	80.79	-	81.76	-
NH_4-N	mg/L	269	22	281.67	6.51
TP	mg/L	17.12	1.53	28.27	1.23

3.2.3. Biomass enrichment strategy

The enrichment culture (refer to Exp. 3) would acclimate to glucose/glycerol bioconversion and CO_2 environment through biomass removal and feeding a fresh substrate solution. The enrichment strategy was based on the substitution of the fresh substrate with the substrate-depleted broth as well as fresh CO_2 headspace. The biomass withdrawal phase and substrate feeding phase were executed in sequence to start a new cycle. The enrichment proceeded with four cycles for 61 days in total, and the final broth was processed and further exposed to 5 bar pCO_2.

Based on the calculation (Appx. 2) of the final biomass requirement, 2-Liter Duran glass bottles were used to acquire enough dry biomass weight for four high-pressure reactors (three experimental replicates and one control). The inoculation principles (Appx. 1) were kept the same as other batch fermentation experiments. During the biomass withdrawal phase, 240 mL of liquid (1200 mL in total) was removed, followed by the substrate feeding phase; the reactor was compensated with a fresh medium consisting of 1 g COD/L substrate and nutrients.

The operation of the reactor was designed to be a 7-days batch cycle since the intermediate metabolites were depleted around 7 days from the preliminary experiments. The duration of each cycle became dependent on the moment when the substrate and its intermediate metabolites were finished; the length of each cycle was 7 days (for the first and second cycle), 21 and 26 days (for the third and fourth cycle); the biomass growth was not as fast as calculated, so the length of third and fourth cycle became longer. Besides, the headspace was fed with 0.3 bar pCO_2 at the beginning of

the first three cycles and 1 bar pCO_2 as the final boost.

The biomass recovery was performed after the fourth-cycle enrichment. The liquid part was first centrifuged using a Heraeus™ Labofuge™ 400 Centrifuge (Thermo Scientific, US) and re-suspended with nutrient solution. Flow cytometry analysis (FCM) was carried out to estimate the cell number. According to the results, the substrate concentration was adjusted to have the final I:S ratio of 2:1 in the pressurized reactors.

3.3. Medium

The synthetic stock medium contained the substrate (1 g COD/L glucose or glycerol), buffer (100 mM $NaHCO_3$), macro and micro-nutrients. Macro and micronutrients solutions were prepared according to the recipe displayed in Table 4.

Table 4. Composition of the macro and micro-nutrient stock solutions[54]

Macronutrient solution			Micronutrient solution		
Compound	Unit	Value	Compound	Unit	Value
NH_4Cl	mg/L	170	$FeCl_3.4H_2O$	mg/L	2
$CaCl_2.2H_2O$	mg/L	8	$CoCl_2.6H_2O$	mg/L	2
$MgSO_4.7H_2O$	mg/L	9	$MnCl_2.4H_2O$	mg/L	0.5
			$CuCl_2.2H_2O$	mg/L	30
			$(NH_4)6Mo7O_2.4H_2O$	mg/L	0.09
			$Na_2SeO_3.5H_2O$	mg/L	0.1
			$NiCl_2.6H_2O$	mg/L	0.05
			EDTA	mg/L	1
			$ZnCl_2$	mg/L	50
			HBO_3	mg/L	0.05
			HCl 36%	mL/L	1

3.4 Reactor setup

Due to the initial starting gas pressure, two types of reactors were employed: Atmospheric Batch Reactor and Pressurized Batch Reactor.

3.4.1 Atmospheric Batch Reactor (ABRs)

The experiments at atmospheric conditions (i.e., 0.3 and 1 bar pCO_2) were carried out in 250-mL Duran glass bottles, air-tight sealed with rubber stoppers. Based on the

inoculation principle (i.e., Gas: Liquid ratio=2:3), the reactors where be operated with 150 mL of the liquid phase and 100 mL of the gas phase. Fig. 8 provides a schematic representation of the experimental setup in atmospheric pressure experiments.

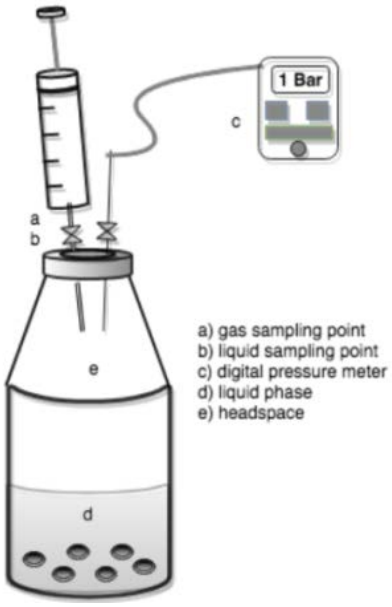

Figure 8. The schematic representation of experimental setup for ABRs [28]

3.4.2 Pressurized Batch Reactors (PBRs)

The experiments at pressurized conditions (i.e., 3 bar, 5 bar and 8 bar) were carried out in pressure-resistant stainless-steel vessels (Nantong Feiyu Petroleum Technology Development Co., Ltd Zhang Yonggen, China) with a total volume of 200 mL. The reactors were fitted with liquid and gas sampling ports, as well as manual glycerine manometers (T-meter®, Centrocom, France). The pressurized experiments were conducted with 120 mL of the liquid phase and 80 mL of the gas phase in the reactor. A schematic representation of this experimental setup for the pressurized condition experiments is displayed in Fig. 9.[51]

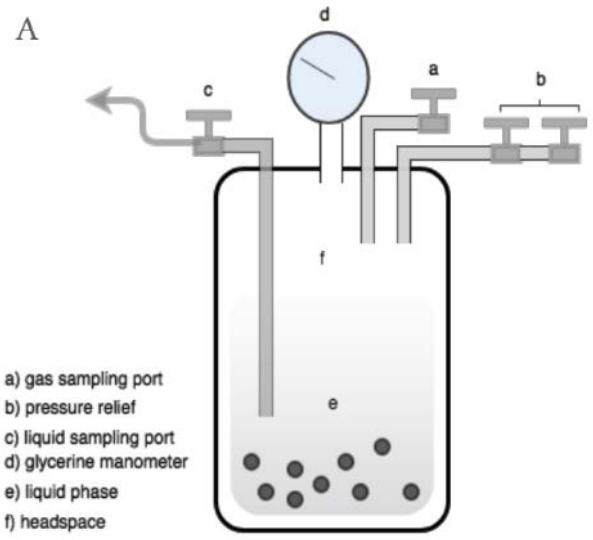

Figure 9. The schematic representation of experimental setup for PBRs [28]

3.5 Reactor operation

Atmospheric and pressurized experiments were conducted in batch mode. Each substrate was tested under 5 different initial pCO_2, namely 0.3, 1, 3, 5, 8 bar according to the previous research, aiming at understanding the effect of increased pCO_2 on glucose and glycerol degradation.

The same inoculation principles (Gas to liquid ratio: 1:1.5; I:S ratio: 2:1) were used for all the batch reactor inoculation. Details about the volume of stock substrate solution and inoculum are provided in Table 5 and 6. On the other hand, headspace supplementation was supplied by following the available internal protocol[55]. In brief, the two experimental set-ups started with 2-minute nitrogen (>99%) flushing to release the oxygen in the reactors; afterward, the CO_2 supplementation was executed. ABRs were flushed either with a gas mixture of 30% N_2/ 70% CO_2 or 100% CO_2 respectively for two minutes. The headspace of the PBRs was subjected to "pressurize and depressurize" method, which was done to ensure complete headspace replacement. The reactors were pressurized to the desired pressure for 2 minutes and slowly depressurized immediately twice, and the CO_2 was kept at the third consecutive pressurization.

ABRs and PBRs were kept at mesophilic condition (35°C) and shaken at 130 rpm. Constant temperature and homogeneous mixing were achieved by means of either an incubator shaker (Brunswick Innova® 44/44R, Eppendorf, Germany) or a static

incubator (Thermo Scientific, France) fitted with orbital and linear motion shaker (ROTABIT, JP SELECTA S.A., Spain).

Table 5. Overview of the experimental conditions applied for glucose and glycerol anaerobic conversion in ABRs and PBRs with elevated pCO_2

Exp. No.	Inoculum type	Substrate type	pCO2 (bar)		Exp. Duration (hr)	Initial substrate con. (g COD/L)	Reactor volume (L)	Principle 1: Gas: Liquid=2:3 Principle 2: I:S=2:1			COD Input (mg)
								Liquid volume (L)		Headspace (L)	
			Initial	Equil.				Substrate	Inoculum		
U0.3	Non-enriched inoculum	Glucose	0.30	0.25	233.0	1	0.25	0.130	0.020	0.100	130.22
U1			1.00	0.99	236.5						
U3			3.00	1.25	236.0		0.20	0.106	0.014	0.080	105.64
U5			5.00	2.39	236.0						
U8			8.00	4.53	232.0						
Y0.3	Non-enriched inoculum	Glycerol	0.30	0.21	236.0	1	0.25	0.130	0.020	0.10	130.22
Y1			1.00	0.99	236.0						
Y3			3.00	1.37	237.5		0.20	0.106	0.014	0.080	105.64
Y5			5.00	2.56	236.5						
Y8			8.00	4.47	241.0						

Table 6. Overview of the experimental conditions applied for glucose and glycerol anaerobic conversion in ABRs and PBRs with elevated pCO2 (Cont'd)

Exp. No.	Inoculum type	Substrate type	pCO2 (bar)		Exp. Duration (hr)	Initial substrate con. (g COD/L)	Reactor volume (L)	Principle 1: Gas: Liquid=2:3 Principle 2: I:S=2:1			COD Input (mg)
								Liquid volume (L)		Headspace (L)	
			Initial	Equi.				Substrate	Inoculum		
UE: 0th cycle	Enriching inoculum	Glucose	0.30	-	168.0	1.00	2.0	1.04	0.158	0.8	1041.00
UE: 1st cycle			0.30	-	168.0	3.60		0.24	0.96	0.8	864.00
UE: 2nd cycle			0.30	-	168.0			0.24	0.96	0.8	864.00
UE: 3rd cycle			0.30	-	504.0			0.24	0.96	0.8	864.00
UE: 4th cycle			1.00	-	624.0			0.24	0.96	0.8	864.00
U5E	Glucose-enriched inoculum	Glucose	5.00	2.55	257.0	1.05	0.2	0.11	0.014	0.08	100.97
YE: 0th cycle	Enriching inoculum	Glycerol	0.30	-	168.0	1.00	2.0	1.04	0.158	0.8	1041.00
YE: 1st cycle			0.30	-	168.0	3.60		0.24	0.96	0.8	864.00
YE: 2nd cycle			0.30	-	168.0			0.24	0.96	0.8	864.00

YE: 3rd cycle			0.30	-	504.0			0.24	0.96	0.8	864.00
YE: 4th cycle			1.00	-	624.0			0.24	0.96	0.8	864.00
YE	Glycerol-enriched inoculum	Glycerol	5.00	2.60	230.5	1.24	0.2	0.11	0.014	0.080	126.83

3.6 Sampling and measurements

To show the reproducibility of the results, five different experimental pCO_2 were run in triplicates. Three units of reactors (X-1, X-2, X-3) are assigned to different sampling purposes to reduce experimental effort as well as to verify the effect of frequent sampling (Fig. 10). Unit X-1 was designed to take liquid samples (2 mL each sample to a maximum number of 10-12 samples, which represent less than 10% of total liquid volume). Unit X-2 was designated for gas sampling (5 mL sample each time, and 3 to 5 times in total). Unit X-3 was used as a reference, taking only 3 liquid and gas samples (at the beginning, middle, and end of the experiment). In this way, the raw data become easier to process since the headspace increment from liquid sampling and pressure losses from gas sampling are necessary to consider. X-1 must compensate only liquid sampling, and X-2 must compensate for gas sampling.

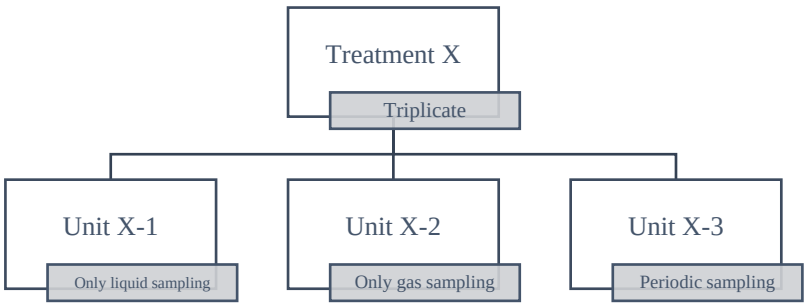

Figure 10. Experimental treatment design

The liquid samples (2 mL) from ABRs and PBRs were centrifuged by means of a MiniSpin® (Eppendorf AG, Germany) at 10000 rpm for 2 mins to separate the solid and liquid. The liquid fraction was filtered with 0.45 μm CHROMAFIL® syringe filters (MACHEREY-NAGEL, Germany), stored at 4℃ and measured within 10 days to minimize the error. In the meantime, the remaining pellets were stored at -80℃ after the liquid part was taken out for the later DNA extraction. Gas samples were taken from ABRs and PBRs using gas-tight syringes and measured within 1 hour. The pressure was recorded before and after sampling for further calculations.

The production of VFAs in the liquid samples was monitored by gas chromatography (7890A GC; Agilent Technologies, USA). The operational conditions were as follows: flame ionization detector (FID) operated at 240°C, oven temperature of 80°C, injection temperature of 120°C and an Agilent 19091F-112 (25m x 0.32mm x 0.5μm) glass column. Helium was used as the carrier gas at a constant flow of 2.4575 ml. min^{-1}[151]. Substrate concentration (i.e., glucose and glycerol), as well as other organic acids such

as lactate and succinate were analyzed by High-performance liquid chromatography (SHIMADZU, Japan). The device was operated with LC-20ATpump (flow rate: 0.6 mL/ min; T= 50 °C), SIL-20A autosampler, CBM-20A controller, CTO-20AC column oven, Aminex HPX-87H column (300 x 7.8 mm), and RID-20A and SPD-20A detectors.

On the other hand, the gas composition was determined via gas chromatography (7890A GC, Agilent Technologies), operated at an oven temperature of 45°C, by directing the samples over an Agilent HPPLOT Molesieve GC column (30m x 0.53 mm x 25 μm) with helium as the carrier gas, which was provided at a constant flow of 10 mL/min. Detection took place by a thermal conductivity detector (TCD) operated at 200°C[51].

To determine the biomass growth, two different methods were applied: volatile suspended solids (VSS) measurement by following Standard Methods[56] and cell counting by flow cytometer (FCM). Although VSS measurement is a widely used method in water treatment research, FCM is another proxy of biomass growth. It also enables better interpretation of amplicon sequencing data since it provides important cell number data without the confounding complications of organic matter[57]. FCM was performed using a BD Accuri® C6 flow cytometer (BD Accuri® cytometers, BD Biosciences, Belgium), and the data was processed with BD Accuri™ C6 software (BD Biosciences, Belgium). Before the measurement, sample pre-treatment was done as follows: dilution with 0.22-μm filtered phosphate-buffered-saline (PBS) solution, then the diluted sample was sonified with Branson Digital Sonifier® 450 (BRANSON Ultrasonics Corporation, US) in 3 cycles of 45 seconds at 100 W and the amplitude at 50%. The pre-treated samples were measured with the flow cytometer after the sample preparation for total and viable cell count: to 495 μL of the pre-treated samples 5 μL of SYBR Green I (SG - total) or SYBR Green + Propidium iodine solution (SGPI - viable) were added.

Other chemical analyses, soluble COD (sCOD) and pH, were performed according to Standard Methods[56].

3.7 Microbial community analysis (MCA)

To examine the effect of elevated pCO_2 on the microbial community and the adaptability to elevated pCO_2, samples were taken from the experimental units presented in Table 6.

Table 7. The analyzed samples of microbial analysis (UE: the glucose-enriched inoculum; YE: the glycerol-enriched inoculum)

Substrate	Baseline	Elevated pCO_2	Adaptability
Glucose	U0.3	U3, U5, U8	UE, UE5
Glycerol	Y0.3	Y3, Y5, Y8	YE, YE5

DNA was extracted using a DNA extraction kit (DNeasy Ultraclean Microbial Kit QIAGEN, QIAGEN, The Netherlands). To increase the representation of microbial community composition, three samples of experimental units (i.e., X-1, X-2, and X-3) were combined during the DNA extraction.

DNA amplification and Illumina sequencing were executed by the DNA sequencing company, Novogene (Hong Kong). According to their internal protocol, during the amplification, DNA concentration and purity were first monitored on 1% agarose gels and diluted to 1ng/μL by sterile water. Then, 16S rRNA genes of distinct regions (16SV3-V4) were amplified with specific primer (e.g. 16S V4: 515F-806R). All PCR reactions were carried out with Phusion® High-Fidelity PCR Master Mix (New England Biolabs). The chosen PCR products, between 400 to 450 bp, were mixed in equidensity ratios. Then, the mixture of PCR products was purified with the Qiagen Gel Extraction Kit (Qiagen, Germany). The libraries of the samples, generated with NEBNext® UltraTM DNA Library Prep Kit for Illumina and quantified via Qubit and Q-PCR, were analyzed by the Illumina platform.

Paired-end reads were assigned to samples based on their unique barcode and truncated by cutting off the barcode and primer sequence. Paired-end reads were merged by FLASH[58], and quality filtering on the raw tags was performed under specific filtering conditions to obtain the high-quality clean tags[59] with the Qiime quality-controlled process [60]. The effective tags were obtained after comparison with UCHIME algorithm[61], the reference database, to detect chimera sequences and subsequent removal of those.

Sequences analysis was performed by Uparse software[62], using all the effective tags. Sequences with ≥97% similarity were assigned to the same operational taxonomic units (OTUs). The representative sequence for each OTU was screened for further annotation. For each representative sequence, Mothur software was performed against the SSUrRNA database of SILVA Database[63] for species annotation at each taxonomic rank (Threshold:0.8~1)[64] (kingdom, phylum, class, order, family, genus, species). To get the

phylogenetic relationship of all OTUs representative sequences, the MUSCLE algorithm[65] was applied to compare multiple sequences. OTUs abundance information was normalized using a standard of sequence number corresponding to the sample with the least sequences.

3.8 Methane production analysis

The methane production was calculated based on the measurements of gas composition (ratio) from GC and the digital pressure meter (GMH3151, GREISINGER, Germany). First, the measurements of the gas composition were calibrated by deducting the oxygen and nitrogen proportionally (O_2: N_2= 1: 3.73) and redistributed again to obtain the exact CO_2, N_2 and CH_4 ratio. Second, the gas pressure measurements were calibrated with reducing the liquid volume and missing moles for gas samplings to know the exact gas pressure without sampling influence. Lastly, the methane production was known through the sum of methane in both gas phase and liquid phase, where the dissolved methane was calculated with the Henry constant ($k_{H,\,35°C}$: 0.0012 mol/L bar).

3.9 Biomass growth analysis

The biomass growth analysis was mainly based on the FCM data, and the measurements were the same in Table 6. In BD Accuri™ C6, density plots were presented with specific fluorescence FL1-H (x-axis) and FL3-H (y-axis). Plots with time on the x-axis and cell counts in the y-axis were employed to detect the background and clogging.

The viable cell counts were obtained with Eq. 5, and this number was also used for COD balance. The counts were converted into the unit of mg COD with Eq. 6 and Eq. 7[57], following the methodology proposed by Brown *et.al* [57].

$$\text{Viable cell}\left(\frac{\text{cell}}{\mu\text{L}}\right) = PolygonCount_{SG}\left(\frac{\text{cell}}{\mu\text{L}}\right) - PolygonCount_{SGPI}\left(\frac{\text{cell}}{\mu\text{L}}\right) \quad \text{(Eq. 5)}$$

$$\text{Biomass growth}\left(\frac{\text{cell}}{\mu\text{L}}\right) = \text{X} = \text{Viable cell (Final count)} - \text{Viable cell (Initial count)} \quad \text{(Eq. 6)}$$

$$\text{Biomass growth(mg VSS)} = \text{X} * \left(\frac{0.25\,(\mu m^3) * 310\,(fg\ C\ \mu m^{-3}) * 10^{-12}}{0.53}\right) \quad \text{(Eq. 7[57])}$$

3.10 Overall stoichiometry analysis

According to the methodology proposed by Rittmann *et.al*[66], energy reactions were

constructed with the relative proportion of electron equivalent represented by each of the reduced end products. The electron equivalents of each product were first computed, then the sum was taken (Ex. 1). Afterward, the fraction that both electron-donor substrates and electron-acceptor products of the total was computed (Eq. 8 and 9). and represent the acceptor and donor's half-reaction of the compound. Finally, the relation (Eq. 10) was applied to obtain the overall stoichiometries.

$\frac{1}{4}CO_2 + H^+ + e^- = \frac{1}{24}C_6H_{12}O_6 + \frac{1}{4}H_2O$;

Glucose donates $24\frac{e^-eq}{mol}$ when it is consumed. When the system consumes 2 moles of glucose, $equiv_{di} = 24 * 2 = 48\ e^-eq$ (Ex. 1)

$R_a = \sum_{i=1}^{n} e_{ai}\, R_{ai}$, where $e_{ai} = \frac{equiv_{ai}}{\sum_{j=1}^{n} equiv_{aj}}$ and $\sum_{i=1}^{n} e_{ai} = 1$ (Eq. 8)

$R_d = \sum_{i=1}^{n} e_{di}\, R_{di}$, where $e_{di} = \frac{equiv_{di}}{\sum_{j=1}^{n} equiv_{dj}}$ and $\sum_{i=1}^{n} e_{di} = 1$ (Eq. 9)

$R_e = R_a - R_d$ (Eq. 10)

Where:
ai: The compounds accepting an electron
e_{ai}: The fraction of the n reduced end products that is represented by product ai
$equiv_{ai}$: The equivalents of ai produced
R_{ai}: The electron acceptor in the half-reaction
R_a: The half-reaction for the electron acceptor
ai: The compounds donating an electron
e_{ai}: The fraction of the n oxidized end products that is represented by product ai
$equiv_{ai}$: The equivalents of ai produced
R_{ai}: The electron donor in the half-reaction
R_a: The half-reaction for the electron donor

3.11 Thermodynamic analysis

The thermodynamic analysis was carried out to verify the feasibility of each biochemical reaction. ΔG^0 (Standards Gibbs free energy change) is the standard value of each reaction at pH 7 and STP condition. ΔG^{01} corresponds to the value corrected with the proton correction by using Eq. 11. ΔG^1 corrects with the real concentration by using Eq. 12; the operational temperature and elevated pCO_2 conditions were calibrated with Eq. 13 to obtain $\Delta G(T', P')$.[67]

$$\Delta G^{01} = \Delta G^0 + R \cdot T \cdot \ln[(1 \times 10^{-7})^{Y_H}] \quad \text{(Eq. 11)}$$

$$\Delta G^1 = \Delta G^0 + R \cdot T \cdot \ln X \quad \text{(Eq. 12)}$$

$$\Delta G(T', P') = \Delta G^0(Ts) * \left(\frac{T'}{Ts}\right) + \Delta H^0(Ts) * \left(\frac{T'-Ts}{Ts}\right) + Y_{CO_2} * R * Ts * \ln\left(\frac{Initial\ pCO_2}{Equil.\ pCO_2}\right) \quad \text{(Eq. 13)}$$

Where:

ΔG^0: free energy change at standard conditions

ΔG^{01}: free energy change at standard conditions and pH 7

ΔG^1: actual free energy change

R: gas constant (0.008314 KJ·mol^{-1}·K^{-1})

Y_H: stoichiometric coefficient of the H^+ ion

X: Reaction coefficient, calculated as the product divided by the reactant

For instance, acetoclastic methanogenesis: $X = \frac{pCH_4 \times pCO_2}{[Ac^-][H^+]}$

T_s: Standard temperature in Kelvin = 298K

Y_{CO2}: stoichiometric coefficient of the CO_2

4. Results

4.1. Effect of elevated pCO2 on the final product spectrum of the fermentation

In the glucose and glycerol fermentation of NEI (Fig. 11), the carbon flux of the measured compounds, as well as the remaining propionate increased with the elevated pCO2, became more complete. The elevated pressure might increase the difficulty of degrading propionate. Moreover, glycerol fermentation had a higher propionate accumulation than glucose: 61% and 39%, respectively. Compared to U5/ Y5, the propionate contribution to the final COD flux in U5E/ Y5E became smaller, while the methane one, got increased. From the obtained results, the enriched inoculum could be more adapted to degrade propionate.

The amount of biomass growth in both fermentations was calculated with the theoretical biomass growth since the measurements of FCM and volatile suspended solids could not draw a conclusive result. The percentage of carbon flux in U5 surpassed 100% when using VSS measurement, while the percentage of carbon flux in Y8 surpassed 100% when using FCM measurement.

Compared to glucose fermentation, glycerol had a relatively lower carbon flux towards the category “other” which means the produced compound other than propionate, butyrate, and acetate became lower. The sludge was mentioned to come from the food waste industry, and thus, the consortium was probably more adapted to consume glucose than glycerol. Therefore, when stress encounters, CO_2 in this case, glucose has more supporting microorganisms, and this caused the higher formation of undefined metabolites (named Other in Fig. 11) in the glucose fermentation.

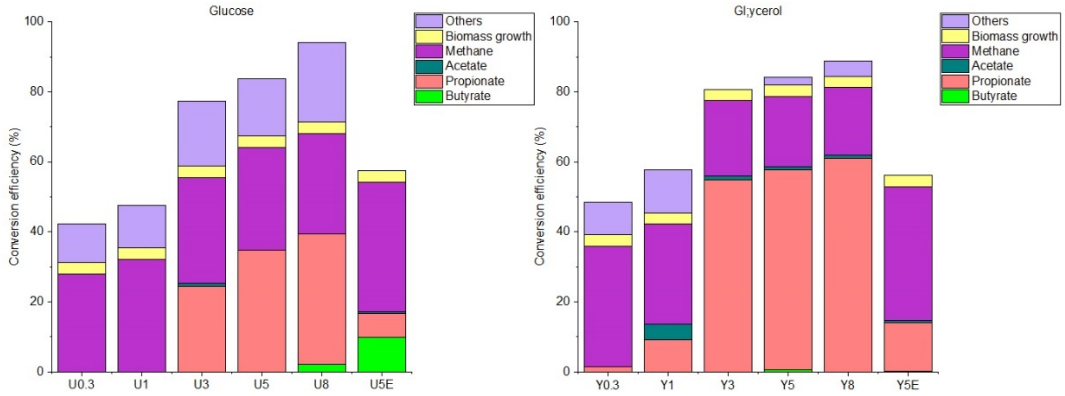

Figure 11. The distribution of the COD flux of each compound in the glucose fermentation (left) in the glycerol fermentation (right) at T=35℃ under 0.3 (U0.3, Y0.3), 1 (U1, Y1), 3 (U3, Y3), 5 (U5, Y5), 8 (U8, Y8) bar initial pCO_2. (Other: the remaining unmeasured COD in the liquid broth; the measurement of sCOD subtracted the final concentration of the measured compounds.)

4.2. Intermediate metabolite formation

4.2.1. Glucose fermentation in ABRs

The result of the intermediate metabolite formation can be categorized into two phases, the production phase, and the degradation phase. The production phase corresponds to the data points before the peak point, and the degradation phase to the data points after the peak. As seen in Fig. 12, the propionate production was predominant in U0.3 and U1, and it was degradable in both conditions. We can see the propionate production phase of U0.3 was as fast as U1, and both productions reached 57 mg COD as well, 44% of the initial COD input. However, the degradation phase of propionate in U1 was longer than U0.3, so the lag phase of the metabolism of propionate-oxidizing metabolism might have occurred.

On the other hand, the concentration of acetate and butyrate were relatively low in the U0.3 and U1. Because of the sampling time, acetate concentration between U0.3 and U1 was slightly different, but the degradation showed small differences. Besides, no butyrate production was observed in the result; therefore, butyrate was either not produced or degraded as fast as the production. The effect of U1 on acetate and butyrate metabolism was akin to U0.3.

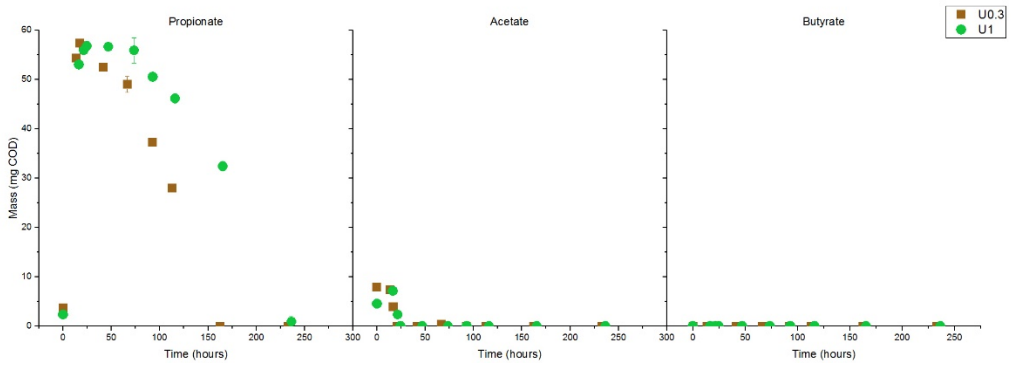

Figure 12. The intermediate metabolite (propionate, acetate, and butyrate) concentrations in glucose fermentation in ABRs, at T=35℃ under 0.3 (U0.3), 1 (U1) bar initial pCO_2.

4.2.2. Glucose fermentation in PBRs

Propionate was still the dominant production in U3, U5, and U8 (Fig. 13). However, the propionate production rate also declined with the elevated pCO_2, and the maximum propionate concentration level decreased to 40 ± 2 mg COD (38% of the initial COD input). On the other hand, the propionate degradation could not be observed in all PBRs. This could be related to the effect of increased pCO2 on the glycolysis or on the pathway from pyruvate to propionate.

With the elevated pCO_2, the acetate production rate also declined, but interestingly, the maximum acetate concentration was ascending. The maximum acetate concentration reached 8.77, 9.62, 16.76 mg COD (8%, 9%, 16% of the initial COD input) in U3, U5, U8, respectively. Moreover, the elevated pCO_2 affected acetate degradation. The acetate was completely consumed in all glucose fermentation experiments except U8, but acetate in U8 was still in the trend of consumption. Besides, butyrate appeared in PBRs, and the concentration also increased with the elevated pCO_2. The butyrate was degradable in PBRs until 8 bar pCO_2.

On the other hand, U5E showed an even lower level of propionate concentration (20.47 mg COD, 20% of the initial COD input); however, U5E enabled propionate to be degraded. The propionate degradability in Y5E was triggered by the enriched inoculum. In this fermentation, the degradation and production of propionate might have happened simultaneously. Meanwhile, butyrate was also produced and accumulated at around 8 mg COD (8% of initial COD input) in U5E but in U5 not.

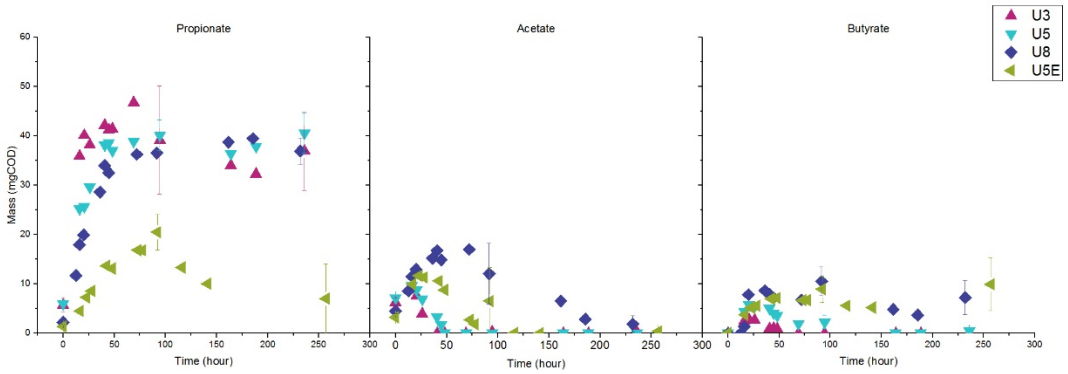

Figure 13. The intermediate metabolite (propionate, acetate, and butyrate) concentrations in glucose fermentation in PBRs, at T=35℃ under 3 (U3), 5 (U5), 8 (U8) bar initial pCO_2.

4.2.3. Glycerol fermentation in ABRs

Propionate dominates the metabolite production in Y0.3 and Y1 (Fig. 14). Y1 (121.65 mg COD, 115% of the initial COD input) had a higher maximum propionate concentration than Y0.3 (86.45 mg COD, 82% of the initial COD input), where Y1 had already surpassed the initial COD input. However, this could be attributed to the measurement error, where the neighboring data points were at a lower level than that data point. Although the production phase could hardly observe the difference between Y0.3 and Y1, the degradation phase of Y1 was not as fast as Y0.3.

On the other hand, little acetate and barely any butyrate were produced in the ABRs. Therefore, either Y0.3 or Y1 did not militate acetate metabolism. Besides, in terms of the butyrate concentration, it was either not produced or not degraded as fast as the production.

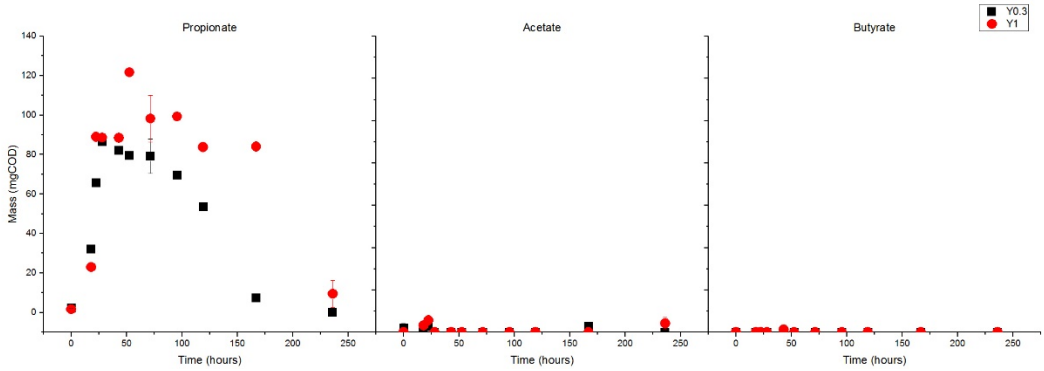

Figure 14. The intermediate metabolite (propionate, acetate, and butyrate) concentrations in glycerol fermentation in ABRs, at T=35℃ under 0.3 (Y0.3), 1 (Y1) bar initial pCO_2.

4.2.4. Glycerol fermentation in PBRs

The slope of the propionate data points during the production phase (Fig. 15) also decreased with the elevated pCO_2. Similarly, propionate degradation got inhibited in Y3, Y5, and Y8, and it accumulated at the concentration of 60-70 mg COD (57-66% of the initial COD input). The level of production and accumulation was higher than U3, U5, and U8, which could be attributed to the higher reducing equivalents produced from glycerol fermentation.

On the other hand, the maximum acetate concentration reached 12.09, 16.65, 15.04 mg COD (11, 16, 14% of the initial COD input) in Y3, Y5, Y8, respectively. These percentages were higher than in the glucose fermentation (8%, 9%, 16% of the initial COD input). Similarly, the elevated pCO_2 affected acetate degradation. It was completely consumed in all glycerol fermentation batch experiments except Y8, but the acetate in Y8 was still in the trend of consumption.

Resembling U5E, Y5E showed a similar pattern where a lower level of propionate concentration (60.68 mg COD, 48% of the initial COD input) than Y3, Y5, and Y8 was seen, and propionate became degradable in the enriched inoculum. The propionate degradability in Y5E was triggered by the enriched inoculum. Therefore, the low concentration might arise from the enriched consortium developing a good syntrophic mechanism of degradation to high-CO_2-content conditions. Although the maximum acetate concentration (21.41 mg COD, 20% of initial COD input) was higher than Y5, the concentration of degradable propionate was higher than the increment in the acetate concentration. This showed that the higher acetate concentration could partially come from the contribution of propionate conversion, and partially come from the less abundant acetate-oxidizing bacteria after the enrichment.

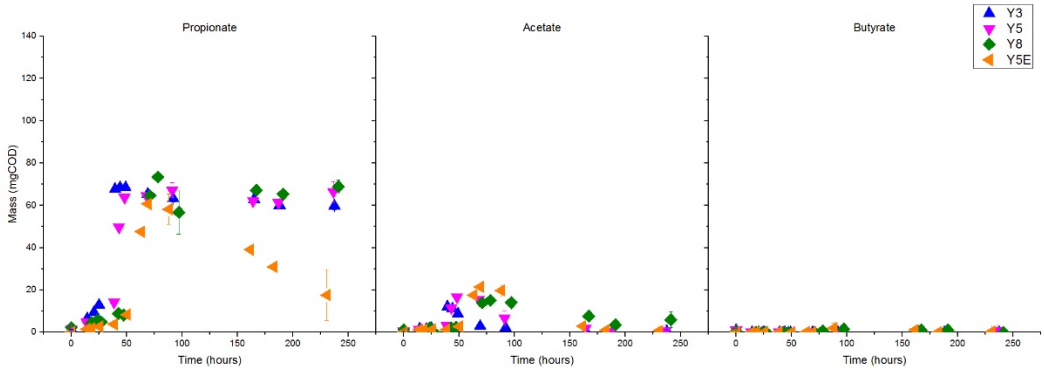

Figure 15. The intermediate metabolite (propionate, acetate, and butyrate) concentrations in glycerol fermentation in PBRs, at T=35°C under 3 (Y3), 5 (Y5), 8 (Y8) bar initial pCO_2.

4.3. Methane production

4.3.1. Glucose fermentation

With elevated pCO_2, no significant distinction of the methane production trend in glucose fermentation occurred among different elevated pCO_2, where most of the data points stayed close, and some of the error bars overlapped with each other. Moreover, the data points increased quite linearly except U0.3. (Fig. 16A). Especially the last data point of U0.3 showed a relatively larger standard deviation (STD), and this could be due to measurement error.

If we pick the upper bond as the last data points of U0.3, we can observe that the production in ABRs (U0.3 and U1) was higher than PBRs (U3, U5, and U8). It is known that part of the methane production in AD relies on the produced hydrogen from intermediate metabolite oxidation (hydrogenotrophic methanogenesis). However, in the PBRs, the propionate degradation was ceased, so it further reduced methane production. U5E, where the propionate-degradable condition was established, had a higher methane production than the other PBRs, which proved the impact of undegradable propionate.

The methane conversion efficiency is the ratio of methane production and the available COD in the reactors (Table 7), which represented how much the methane can be formed with the amount of available COD. Based on the COD balance, the initial COD input will be converted into different products, such as VFA, CH_4, biomass and so on. The available COD is considered as the initial COD input minus the amount of COD consumed/remained in other compounds in the final product spectrum except CH_4 ; Despite that it does not relate to the actual measurement of methane production, the conversion efficiency increased with the elevated pCO_2 in the NEI. The increasing conversion efficiency can be due to the increasing acetate production with elevated pCO_2 discussed in Section 4.2, and further generated more methane. On the other hand, the increasing conversion efficiency can also be due to the extra methane production from hydrogenotrophic methanogenesis. The increased pCO_2 raised the concentration of available dissolved CO_2 in PBRs, which would favor the pathway of homoacetogenesis and/or hydrogenotrophic methanogenesis (ΔG^1_{Hydro}). The methane production from homoacetogenesis should combine with acetoclastic methanogenesis ($\Delta G^1_{Homo + Aceto}$). Based on thermodynamic calculations, both pathways have the same

ΔG^1 value, being in theory, equally favorable. (ΔG^1_{Hydro}: -17.3 kJ/mol[1]; $\Delta G^1_{Homo + Aceto}$: -17.3 kJ/mol[2]; ΔG^1_{Hydro}: -25.8 kJ/mol[3]; $\Delta G^1_{Homo + Aceto}$: -25.8 kJ/mol[4])

4.3.2. Glycerol fermentation

Similarly, glycerol fermentation did not demonstrate a clear trend of methane production among the reactors, but the difference of methane production between ABRs (Y0.3, Y1) and PBRs (Y3, Y5, and Y8) in the last data points can be observed (Fig. 16B). The propionate degradation inhibition in the PBRs might result in lower methane production than the ABRs due to the reduction of produced hydrogen from propionate conversion for hydrogenotrophic methanogenesis. Furthermore, Y5E, the propionate-degradable condition, again proved the potential relationship between propionate degradation and methane production. Interestingly, the methane conversion efficiency not only increased with elevated pCO_2 but surpassed the available COD for methane production. This is because CO_2 is not accountable in COD balance, but it could contribute to methane production.

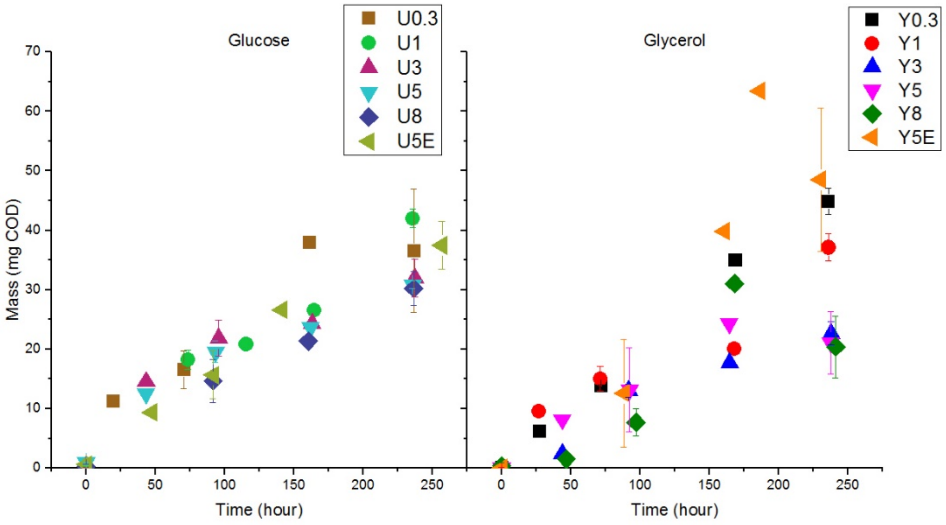

Figure 16. Methane production from glucose and glycerol fermentation at T=35°C under 0.3 (U0.3, Y0.3), 1 (U1, Y1), 3 (U3, Y3), 5 (U5, Y5), 8 (U8, Y8) bar initial pCO_2. (Left: Fig.16A; right: Fig.16B)

[1] The thermodynamic analysis was simulated at the pCO_2 of 0.3 bar, pH of 7.37, temperature of 35°C, and pH_2 of 10^{-4} bar

[2] The thermodynamic analysis was simulated at the pCO_2 of 0.3 bar, pH of 7.37, temperature of 35°C, and pH_2 of 10^{-4} bar; homoacetogenesis and acetoclastic methanogenesis are assumue to be consecutive reactions, so the ΔG values from two individual reactions were summed up.

[3] The thermodynamic analysis was simulated at the pCO_2 of 8 bar, pH of 5.94, temperature of 35°C, and pH_2 of 10^{-4} bar

[4] The thermodynamic analysis was simulated at the pCO_2 of 8 bar, pH of 5.94, temperature of 35°C, and pH_2 of 10^{-4} bar; homoacetogenesis and acetoclastic methanogenesis are assumue to be consecutive reactions, so the ΔG values from two individual reactions were summed up.

4.3.3. The effect of elevated pCO_2 to the methane production

A more significant gap can be seen in the last points of glycerol fermentation between the ABRs and the PBRs compared to glucose fermentation (Fig. 16). This could be related to the inhibition of propionate degradation in the PBRs, where glycerol directs more carbon flux towards propionate. Although methane production is directly affected by the acetate degradation, the undegradable propionate would further affect the methane production. Therefore, the carbon flux for the potential methane production losing in the accumulation of propionate was larger in glycerol than glucose. Moreover, the propionate degradation in U5E and Y5E was not suppressed by the pCO_2, and they showed similar final production as ABRs.

The control reactors helped to differentiate the pressure effect on methane production (Table 7) from the pCO_2 effect. However, this is not in the scope of this research. A relative higher methane production and conversion efficiency happened with elevated pN_2. Pressure has been proposed to have a stabilizing effect on an enzyme or enzymes crucial to methane production[68] or increase the solubility of biologically relevant gases[69], which also potentially dictate the methane production. Correspondingly, the conversion efficiency increased with elevated pCO_2, and thus, we reasonably suppose that the high-pressure and increasing CO_2 jointly affected the methane conversion efficiency.

Table 8. Methanogenesis efficiency with elevated pCO_2 at T=35°C under 0.3, 1, 3, 5, 8 bar initial pCO_2 and 1, 5, 8 bar initial pN_2. (*: Calculated value, where initial COD input minus Biomass growth, and sCOD.)

Initial pCO_2 (Bar)	**Available COD* (mg COD)**	**Methane production (mg COD)**	**Conversion (%)**	**Initial pN_2 (Bar)**	**Available COD* (mg COD)**	**Methane production (mg COD)**	**Conversion (%)**
Glucose fermentation							
0.30	115.83	36.56	31.56	-	-	-	-
1.00	114.51	41.98	36.66	1.00	115.56	30.79	26.64
3.00	59.40	31.99	53.86	-	-	-	
5.00	51.352	30.83	60.04	5.00	87.54	70.23	80.23
8.00	39.907	30.22	75.73	8.00	85.04	69.91	82.21
5.00 (En)	78.32	37.46	47.83	5.00 (En)	90.97	51.64	56.77
Glycerol fermentation							
0.30	110.74	44.84	40.49	-	-	-	-
1.00	96.52	37.01	38.34	1.00	113.43	48.04	42.35
3.00	31.20	22.70	72.76	-	-	-	
5.00	21.97	21.11	96.09	5.00	77.52	59.59	76.87
8.00	6.75	20.39	302.07	8.00	90.14	69.29	76.87
5.00 (En)	109.90	48.51	44.14	5.00 (En)	120.82	87.846	72.71

4.4. Microbial community analysis (MCA)

4.4.1. Substrate affinity of the microbial community

From the calculation of the top 10 genera, not much can be said about substrate affinity; however, it does not mean that general trends cannot be outlined while comparing the relative abundance of NEI, UE, and YE. As seen in Fig. 17, *Methanosaeta*, *Georgenia*, *Methanobacterium*, *Smithella*, and *Thermovirga* got more abundant during the enrichment with glucose, meaning that those microorganisms could be directly or indirectly supported by glucose as substrate. On the other hand, during the glycerol enrichment, *Smithella, Thermovirga, Pseudomonas, and Rhizobium* got more abundant, and *Methanosaeta and Georgenia* stayed the same, meaning that those microorganisms could be directly or indirectly supported by glycerol as substrate.

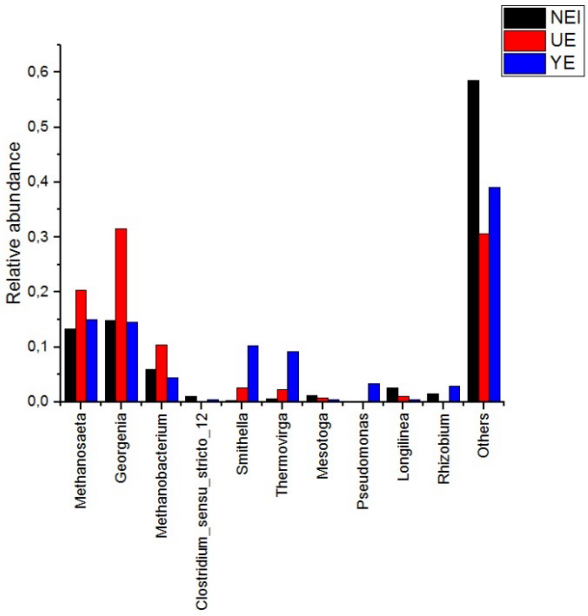

Figure 17. The relative abundance of the non-enriched inoculum and the enriched inoculum

4.4.2. The effect of elevated pCO_2 to the microbial community

To isolate the double effects of substrate affinity and elevated pCO_2, the comparison of MCA was made between the inoculum and the inoculum cultured under 5 bar pCO_2. As seen in Fig. 18, both *Methanosaeta* and *Georgenia* in U5, U5E, Y5, Y5E increased their abundance after being exposed to initial pCO_2 of 5 bar, while *Methanobacterium* only got more abundant in U5 but U5E, Y5, and Y5E. Therefore, we suspect that the initial pCO_2 of 5 bar could be beneficial to *Methanosaeta* and *Georgenia* exclusively. However, *Methanobacterium*, hydrogenotrophic methanogen, was plausible to be

competing for the hydrogen with homoacetogens, where the relative abundance appeared to vary complementarily. One of the groups in the genus of *Clostridium* is homoacetogenic *Clostridia* which has the ability to fix CO_2 via the Wood-Ljungdahl pathway[70]. *Clostridium* acted conversely to the CO_2-exposing condition as U5, U5E, Y5, and Y5E, so we suspect that the genus played a role to compete with *Methanobacterium*.

Moreover, *Smithella*, a microorganism that grows syntrophically on propionate with methanogenic bacteria to remove H_2, appeared in the enriched inoculum (i.e., UE, YE). Therefore, propionate becoming degradable at the initial pCO_2 of 5 bar might be due to the enrichment and adaptation of *Smithella*. Moreover, the abundance of *Smithella* was higher in glycerol fermentation than glucose, which corresponds to the higher production of propionate in glycerol fermentation.

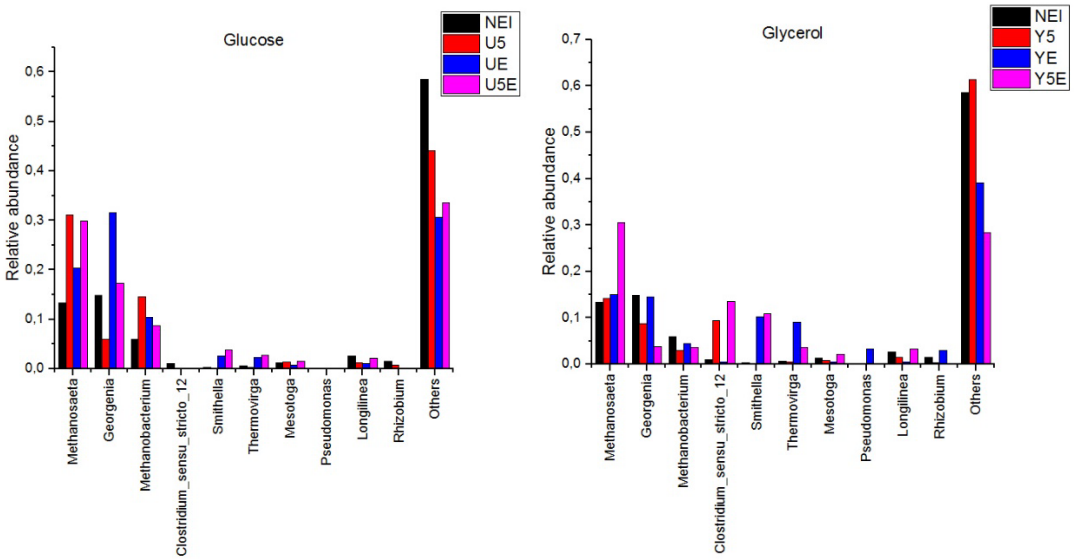

Figure 18. The relative abundance of the non-enriched inoculum (NEI) and the inoculum after exposed to 5 bar pCO_2 initial pCO_2 (U5, Y5); the relative abundance of the enriched inoculum (UE, YE) and the inoculum after exposed to 5 bar pCO_2 initial pCO_2 (U5E, Y5E).

4.4.3. The effect of elevated pCO_2 to the microbial growth

Afterwards, the relative abundance of all the elevated pCO_2 conditions was compared with the baseline conditions, U0.3 and Y0.3, to verify the previously proposed hypothesis on each microorganism. *Methanosaeta* was hypothesized to be indirectly supported by glucose and glycerol as substrate and get more abundant after 5 bar pCO_2 exposure. As seen in Fig. 19, *Methanosaeta* could also overall be enriched with the elevated pCO_2 from glucose as a substrate, and this might due to the increasing acetate

production. Although acetate was still degradable in the experiment, the trend of *Methanosaeta* was opposite in glycerol fermentation, which might be caused by the different interactions between *Methanosaeta* and other microorganisms, such as competitive inhibition. On the other hand, *Georgenia* got less abundant with elevated pCO_2 when using glucose as a substrate instead of glycerol. Regarding this genus, there a limited amount of research on the strain, *Georgenia*. *Georgenia ruanii sp*. uses glucose as sole carbon and energy source[71], and *Georgenia subflava sp. Nov.* can positively oxidize glycerol[72]. Either bacteria were not mentioned to use both substrates, so the specific limitation could not be defined. Nevertheless, Kerfahi *et al.*, revealed a shift in community composition with acidification from increasing pCO_2, and *Georgenia* was relatively more abundant at low pH.[73]

Furthermore, of glycerol fermentation, *Clostridium* was more abundant with the elevated pCO_2, and the phenomenon also happened in YE5. The bacteria under the *Clostridium* genus has a diverse characteristic; homoacetogenic *Clostridium* was suspected to compete with *Methanobacterium* for hydrogen. On the other hand, *Clostridium propionicum* has been reported to use glycerol and/or lactate as a substrate to produce, succinate, acetate, and/or formate [74]. However, the data of the glucose experiment (Fig. 19) does not clearly show the complementary relationship between *Methanobacterium* and *Clostridium*. Therefore, *Clostridium* might only be the competitor in glycerol fermentation, and glucose had other microorganisms to compete with *Methanobacterium*. Meanwhile, *Clostridium* was also plausible to function as propionate-producing bacteria in glycerol fermentation since it only became more abundant with glycerol.

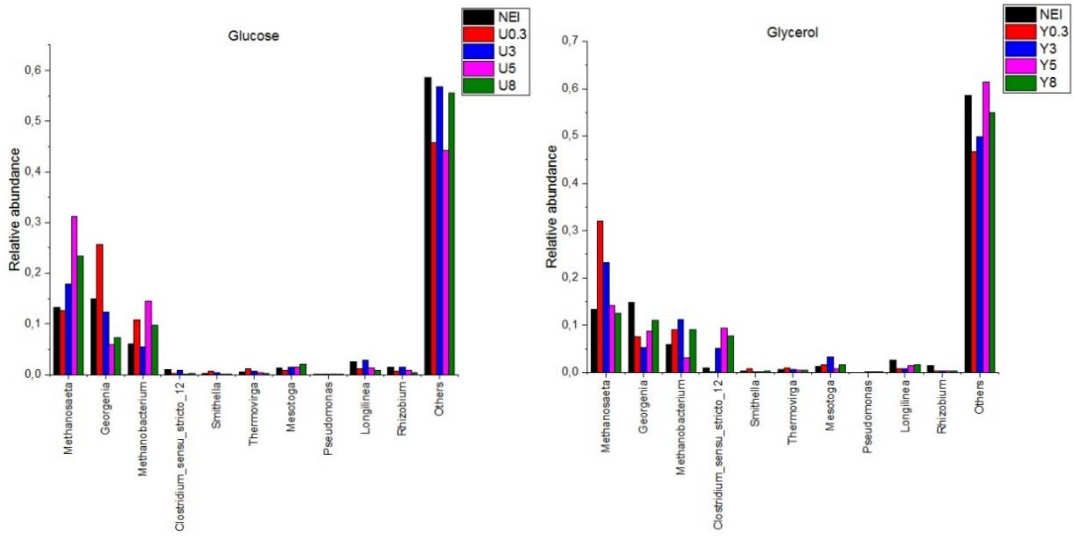

Figure 19. The relative abundance of the non-enriched inoculum (NEI) and the inoculum after exposed to 0.3, 3, 5, 8 bar pCO_2 initial pCO_2 (U0.3, U3, U5, U8); the relative abundance of the non-enriched inoculum (NEI) and the inoculum after exposed to 0.3, 3, 5, 8 bar pCO_2 initial pCO_2 (Y0.3, Y3, Y5, Y8)

4.4.4. The effect of elevated pCO_2 on the cell viability

As seen in Fig. 20, if we neglect the data of U8 and Y8, the difference in viability between glucose and glycerol fermentation can be observed. With the elevated pCO_2, the final cell viability was always lower than the initial cell viability in glucose but glycerol fermentation, which might be due to the property of the substrates. Glycerol has been considered as an ingredient to preserve microorganisms and remain their viability[75]. Therefore, we suspected that glycerol prevented the microorganisms from the CO_2 stress effect, and in consequence, they became more viable. On the other hand, glucose does not have the property of cell protection, and thus, it might cause a reduction of viability.

In Fig. 21, the cell viability after the CO_2 exposure increased in both enriched-inoculum, so the enriched inoculum might become adapted to perform the metabolism under the CO_2-exposing condition. Moreover, the final viability increased in glycerol fermentation since glycerol is the constituent of cell membrane that might prevent the cell from CO_2 stress effect.

In terms of the initial cell viability, it varied irregularly although the samples of initial cell viability were taken right after the inoculum was exposed to certain pCO_2 conditions. Therefore, CO_2 effect might not happen instantly. Nevertheless, the irregularity might be caused by error, which can be emerged during the sample

preparation. On one hand, although the samples were all measured within 24 hours, the samples could not be measured immediately sometimes due to the availability of the equipment. Thus, the strict anaerobes would become non-viable cells as time goes by, causing some minor errors to the measurement. On the other hand, the cell viability was based on the ratio of viable cell count and total cell count, and the measurements were done separately. Sample preparation dealt with small volumes (i.e., 495 uL sample + 5 uL stain); therefore, if any volume error has occurred, it would affect the ratio of viability.

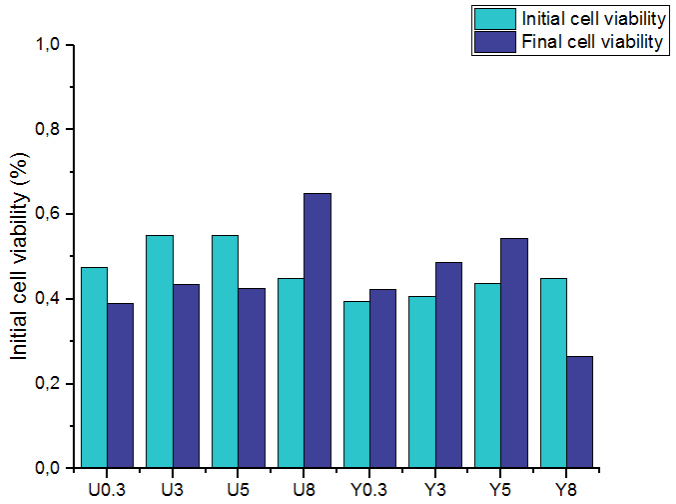

Figure 20. The cell viability of the glucose fermentation in the non-enriched inoculum (NEI) at T=35°C under 0.3 (U0.3), 1 (U1), 3 (U3), 5 (U5), 8 (U8) bar initial pCO_2 and of the glycerol fermentation in the non-enriched inoculum (NEI) at T=35°C under 0.3 (Y0.3), 1 (Y1), 3 (Y3), 5 (Y5), 8 (Y8) bar initial pCO_2

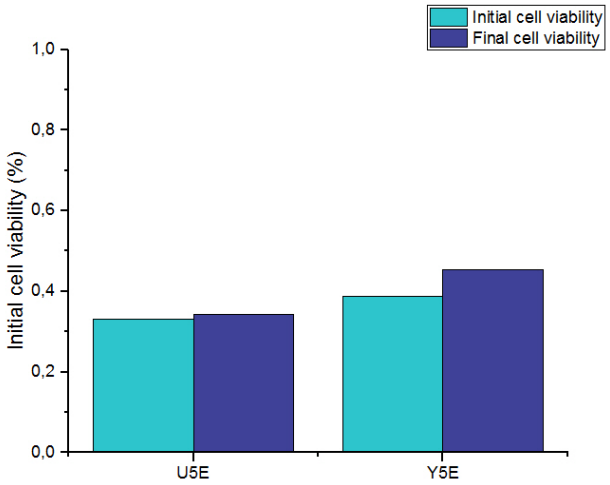

Figure 21. The cell viability of the glucose fermentation in the enriched inoculum (UE) at T=35°C under 5 bar initial pCO_2 (U5E) and of the glycerol fermentation in the enriched inoculum (YE) at T=35°C under 5 bar initial pCO_2 (Y5E).

5. Overall discussion

From this research, we hypothesized that the elevated pCO_2 converged the substrate conversion pathways towards propionate and acetate production, especially propionate (Fig. 12-15). However, the complete carbon flux (Fig. 11) could not be outlined due to presence of unmeasured compounds in the soluble phase.

Based on the variation of propionate concentration, initial pCO_2 of 0.3 bar and 1 bar did not produce visible inhibition on propionate production. Therefore, the conditions might not have caused detrimental effect on both glycolysis and the conversion of pyruvate to propionate. However, the propionate degradation was kinetically affected under 0.3 and 1 bar initial pCO_2. Although the propionate was degradable, the propionate degradation phase at 1 bar initial pCO_2 was longer than 0.3 bar. On the contrary, when the pCO_2 was elevated to 3, 5, and 8 bar, not only the propionate production phase became longer, but also the maximum concentration became lower. The initial pCO_2 of 3, 5, and 8 bar might affect glycolysis and/ or the pyruvate conversion to propionate. Wan *et.al* demonstrated that the increase of CO_2 concentrationdecreased the NADH production by 45.5% in the denitrifying microbe *Paracoccus denitrificans*[46]. Therefore, the NADH might also decrease with the initial pCO_2 at 3, 5, and 8 bar conditions, and further decreased the production of propionate. On the other hand, Wan *et.al* showed that the increasing CO_2 concentration inhibited the carbon source utilization because the growth and viability of denitrifier cells were suppressed by CO_2 effect[46]. Therefore, the higher production of propionate from glycerol fermentation might be caused not only by the available reducing power of the substrate (each c-mole of glucose and glycerol produces 0.33 mole NADH and 0.66 mole NADH, respectively) but also by the cell viability was higher in glycerol fermentation.

Propionate degradation did not occur since the initial pCO_2 of 3 bar. We suspect that the non-degradability might arise from the thermodynamic limitations of the conversion from propionate to acetate. Moreover, this conversion involves a decarboxylation reaction. Under standard conditions, the propionate-oxidation pathway is generally coupled to hydrogenotrophic methanogenesis to consume the produced hydrogen and make the oxidation process energetically feasible.[76] ($\Delta G^1_{\text{propionate oxidation}}$: 39.5 kJ/mol[5];

[5] The thermodynamic analysis was simulated at the pCO_2 of 0.3 bar, pH of 7.37, temperature of 35°C, and pH_2 of 10^{-4} bar

$\Delta G^{1}_{\text{propionate oxidation}}$: 56.5 kJ/mol[6]) We also suspect that the elevated pCO_2 might cause a physiological detrimental effects on the cell structure [77] of the syntrophic partners, namely propionate-consuming bacteria and hydrogenotrophic methanogens, causing the accumulation of the undegradable propionate.

On the other hand, in the enriched inoculum, propionate became degradable at 5 bar initial pCO_2, but the measured concentration was lower than the 5 bar initial pCO_2 in non-enriched inoculum.The low concentration might arise from the efficient syntrophic mechanism of degradation to high-CO_2-content conditions developed by the enriched consortium. Based on the microbial community analysis (MCA), *Smithella* appeared in UE and YE through the enrichment. *Smithella* was mentioned as a syntrophic, propionate-oxidizing bacteria, and thus, the propionate in U5E and Y5E was hypothesized to be degraded by it. Unlike conventional syntrophic propionate oxidization pathway, *Smithella spp.* utilize the dismutation pathway; two propionates are conjoined to a six-carbon intermediate that is dismutated to one acetate and one butyrate.[78,79] Butyrate concentration only appeared in the glucose fermentation, and the ratio of the maximal concentration was nearly 1:1. Since the complex reactions in AD can happen at a relatively fast rate, the exact ratio over time was difficult to monitor. On the contrary, the degradable propionate in Y5E became puzzled because no butyrate was formed.

Theoretically, propionate can be produced through two pathways from pyruvate; either through succinate (succinate pathway) or lactate (acrylate pathway). In the previous research by Gómez Páez[51], pyruvate was prone to convert into propionate, and it was suspected to go through the succinate pathway since it is the only pathway to incorporate CO_2. However, *Clostridium* became more abundant than original inoculum in glycerol fermentation, and the phenomenon also happened in YE5. Axayacatl *et.al* showed that the metabolism of *Clostridium propionicum* follows the acrylate pathway (Fig. 6)[52], and thus, it is suspected that propionate was not only produced through succinate pathway but also acrylate pathway. In fact, the bacteria under the *Clostridium* genus has a diverse characteristic. *Clostridium* was also suspected to act as homoacetogen and competed with *Methanobacterium*. However, the data of glucose experiment (Fig. 19) did not clearly show the complementary relationship between *Methanobacterium* and *Clostridium*. Therefore, *Clostridium* might only be the competitor in glycerol fermentation, and glucose had other microorganisms to compete with *Methanobacterium*. Nevertheless, no strong evidence allowed us to conclude

[6] The thermodynamic analysis was simulated at the pCO_2 of 8 bar, pH of 5.94, temperature of 35°C, and pH_2 of 10^{-4} bar

about the particular functions of *Clostridium* unless the gene expression or other expression techniques is executed.

In terms of acetate, the production phase and degradation phase had no difference among the data points under 0.3 and 1 bar initial pCO_2. Moreover, the consecutive reactions, propionate degradation to acetate and acetate degradation to methane, might be able to cooperate well under the conditions since the increment of acetate concentration did not correspond to the reduction of propionate concentration over time. On the contrary, with the elevated pCO_2, the acetate production phase and the maximum acetate concentration also became longer and higher. The ascending concentration could be attributed to the participation of homoacetogenesis during the production phase, where the increased CO_2 concentration would favor the reaction of homoacetogenesis (ΔG^1_{Homo}). (ΔG^1_{Homo}: 19.8 kJ/mol [7]; ΔG^1_{Homo}: 11.4 kJ/mol [8]) Furthermore, the degradation phase of acetate at 8 bar took 200 hours more to consume most of the acetate. Since the reaction of acetoclastic methanogenesis generates CO_2 as well, it might be effectively affected by the 8 bar initial pCO_2.

Butyrate did not appear in PBRs, and we suspect that the production of butyrate was affected by different properties of the substrates. The butyrate formation from acetyl-CoA needs the participation of reducing power, so the distribution of reducing equivalents from the glycerol fermentation might have not gone towards the butyrate formation pathway; barely any butyrate production can be seen in Y5E as well. On the contrary, butyrate was accumulated in U5E but in U5 not. Although the butyrate-consuming bacteria, such as *Syntrophomonas* [80], was not detected in the MCA, this minor genus might have become less dominant than the NEI after the enrichment.

Besides, methane production did not show a trend among different pCO_2 except for the last data points. The propionate-degradable conditions (i.e., U0.3, U1, U5E, Y0.3, Y1, and Y5E) showed higher methane production than the propionate-undegradable conditions (i.e., U3, U5, U8, Y3, Y5, and Y8). We suspect that the undegradable propionate potentially reduced methane production since the propionate could not be converted. Moreover, a bigger gap of methane production in glycerol fermentation can be observed (Fig. 16), and this might be related to the inhibition of propionate degradation in the PBRs as well. However, the methane production U5E and Y5E was not suppressed by elevated pCO_2 and showed an increased level of methane production,

[7] The thermodynamic analysis was simulated at the pCO_2 of 0.3 bar, pH of 7.37, temperature of 35°C, and pH_2 of 10^{-4} bar

[8] The thermodynamic analysis was simulated at the pCO_2 of 8 bar, pH of 5.94, temperature of 35°C, and pH_2 of 10^{-4} bar

suggesting that the elevated pCO_2 might have caused negligible effect to the methanogens or to the adapted methanogens than the fermentative bacteria.

In the MCA, the elevated pCO_2 and the enrichment did not change the microbial communities entirely since the experimental period was not sufficiently long.

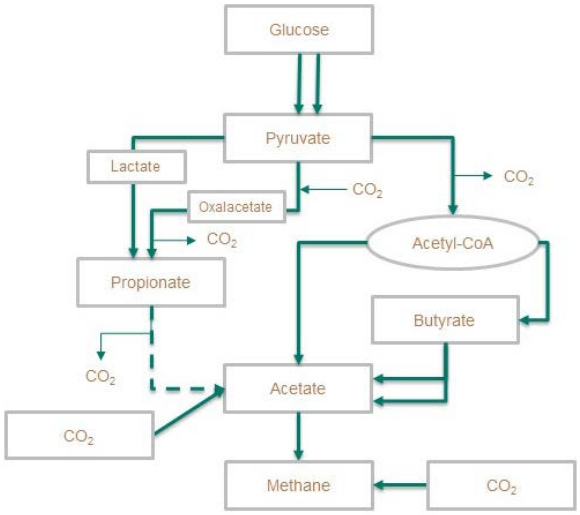

Figure 22. Glucose degradation pathway

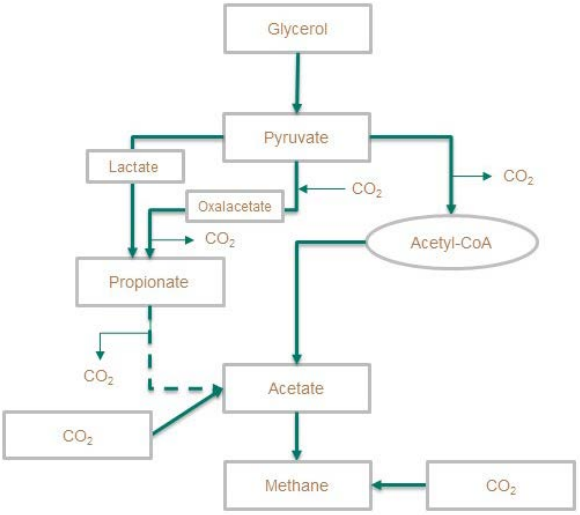

Figure 23. Glycerol degradation pathway

6. Conclusions

This study revealed that the elevated pCO_2 narrowed down the product spectrum of glucose and glycerol fermentation and favored the substrate degradation towards propionate, while the degradation of produced propionate was inhibited from 3 bar initial pCO_2. There were several reasons proposed in the overall discussion section, but more research needs to be carried out to elucidate the effect. The exact propionate-producing pathway could not be confirmed with the MCA and thermodynamic analysis; gene expression needs to be conducted to verify upregulated functions. It was established that after the culture enrichment, propionate became degradable. Base on the MCA, we suspect that *Smithella* played a role in degrading propionate. However, this hypothesis also needs further confirmation at the gene expression level. On the other hand, the difference between the glucose and glycerol fermentation has been revealed in propionate measurements, where the higher reducing power generated higher propionate. The substrate was also hypothesized to influence the cell viability, where glycerol fermentation increased the cell viability compared to glucose. The degradation of acetate and butyrate in the non-enriched inoculum was observed to be kinetically affected by the elevated pCO_2. In the case of butyrate, it became undegradable at 8 bar; however, the particular reason was not determined during this research.

7. Recommendations

This research intended to understand the CO_2 effect on the conversion of the substrates in AD. The nature of anaerobic digestion made the research quite challenging since we needed a large amount of data to draw solid conclusions. The study observed the hypothetical degradation pathway of glucose and glycerol with the elevated pCO_2; however, the exact mechanism that triggered the pathway selection is still undisclosed. Therefore, more research on molecular biology and gene expression under elevated pCO_2 needs to be done. Moreover, to make the technique more applicable in practice, a higher substrate loading rate and the CSTR (continuous stirred tank reactor) with suitable HRT (hydraulic retention time) can be tested to see the possibility of upscaling the technology.

Based on the current methodology, it can be suggested the additional determination of storage polymers, which could allow a more complete COD balance (Section 4.1). On the other hand, the labeled substrate approach (i.e., isotope) can be applied to track the carbon flow. For example, methane production can come from either homoacetogenesis or acetoclastic methanogenesis; however, acetate could be immediately consumed and results in no detection of acetate, causing a wrong hypothesis. Therefore, the use of labeled compound compounds could help to elucidate the metabolic pathways.

From my perspective, high-pressure anaerobic digestion could be a promising technique in the aspects of sustainability. Not only the ability of biorefinery but also the reactor material is more environmentally friendly. Normally, the material of high-pressure systems is stainless steel, and if well maintained, it is more durable compared to plastic and glass used by non-pressure systems. Moreover, this technology can be a tool for CO_2 sequestration and further produce valuable chemical feedstocks. Therefore, in the future, there might be a potential that the waste gases containing CO_2 from industries (e.g., petrochemical industry) can be processed and combined with liquid waste streams to generate valuable end-product by the steer of pCO_2.

Bibliography

1. Dharmadi, Y., Murarka, A. & Gonzalez, R. Anaerobic fermentation of glycerol byEscherichia coli: A new platform for metabolic engineering. *Biotechnol. Bioeng.* **94**, 821–829 (2006).
2. Evren, M., Ozgun, H., Kaan, R. & Ozturk, I. Anaerobic Treatment of Industrial Effluents: An Overview of Applications. in *Waste Water - Treatment and Reutilization* (ed. Garca Einschlag, F. S.) (InTech, 2011). doi:10.5772/16032.
3. Atasoy, M., Owusu-Agyeman, I., Plaza, E. & Cetecioglu, Z. Bio-based volatile fatty acid production and recovery from waste streams: Current status and future challenges. *Bioresource Technology* **268**, 773–786 (2018).
4. Lindeboom, R. E. F. Autogenerative high pressure digestion: biogass production and upgrading in a single step. (2014).
5. Kleerebezem, R., Joosse, B., Rozendal, R. & Van Loosdrecht, M. C. M. Anaerobic digestion without biogas? *Reviews in Environmental Science and Bio/Technology* **14**, 787–801 (2015).
6. *IEA bioenergy Task 42 on biorefineries: co-production of fuels, chemicals,power and materials from biomass. In: Minutes of the third Task meeting*. https://www.iea-bioenergy.task42-biorefineries.com/en/ieabiorefinery.htm (2007).
7. Bowie, C. T. C., Sneddon, D. M. & Montgomery, A. R. Considerations in Design

and Operation of a Biogas Plant. in *Energy for Rural and Island Communities* 371–377 (Elsevier, 1984). doi:10.1016/B978-0-08-030580-6.50049-8.

8. Agler, M. T., Wrenn, B. A., Zinder, S. H. & Angenent, L. T. Waste to bioproduct conversion with undefined mixed cultures: the carboxylate platform. *Trends in Biotechnology* **29**, 70–78 (2011).
9. Lindeboom, R. E. F., Ferrer, I., Weijma, J. & van Lier, J. B. Effect of substrate and cation requirement on anaerobic volatile fatty acid conversion rates at elevated biogas pressure. *Bioresource Technology* **150**, 60–66 (2013).
10. Hansson, G. Methane production from glucose and fatty acids at 55?85�C: Adaption of cultures and effects of pCO2. *Biotechnol Lett* **4**, 789–794 (1982).
11. Muñoz Sierra, J. D., Oosterkamp, M. J., Wang, W., Spanjers, H. & van Lier, J. B. Impact of long-term salinity exposure in anaerobic membrane bioreactors treating phenolic wastewater: Performance robustness and endured microbial community. *Water Research* **141**, 172–184 (2018).
12. Scoma, A. & Boon, N. Osmotic Stress Confers Enhanced Cell Integrity to Hydrostatic Pressure but Impairs Growth in Alcanivorax borkumensis SK2. *Frontiers in Microbiology* **7**, (2016).
13. Arslan, D. *et al.* Effect of hydrogen and carbon dioxide on carboxylic acids patterns in mixed culture fermentation. *Bioresource Technology* **118**, 227–234

(2012).

14. Zhou, M. *et al.* Enhanced carboxylic acids production by decreasing hydrogen partial pressure during acidogenic fermentation of glucose. *Bioresource Technology* **245**, 44–51 (2017).
15. Prescott, L. M., Harley, J. P. & Klein, D. A. *Microbiology*. (McGraw-Hill, 2002).
16. Zacharof, M.-P. & Lovitt, R. W. Complex Effluent Streams as a Potential Source of Volatile Fatty Acids. *Waste Biomass Valor* **4**, 557–581 (2013).
17. Singhabhandhu, A. & Tezuka, T. A perspective on incorporation of glycerin purification process in biodiesel plants using waste cooking oil as feedstock. *Energy* **35**, 2493–2504 (2010).
18. Quispe, C. A. G., Coronado, C. J. R. & Carvalho Jr., J. A. Glycerol: Production, consumption, prices, characterization and new trends in combustion. *Renewable and Sustainable Energy Reviews* **27**, 475–493 (2013).
19. *Biological wastewater treatment: principles, modelling and design*. (IWA Pub, 2008).
20. Batstone, D. J., Picioreanu, C. & van Loosdrecht, M. C. M. Multidimensional modelling to investigate interspecies hydrogen transfer in anaerobic biofilms. *Water Research* **40**, 3099–3108 (2006).
21. Sikora, A., Detman, A., Chojnacka, A. & Blaszczyk, M. K. Anaerobic Digestion:

I. A Common Process Ensuring Energy Flow and the Circulation of Matter in Ecosystems. II. A Tool for the Production of Gaseous Biofuels. in *Fermentation Processes* (ed. Jozala, A. F.) (InTech, 2017). doi:10.5772/64645.

22. Diekert, G. & Wohlfarth, G. Metabolism of homoacetogens. *Antonie van Leeuwenhoek* **66**, 209–221 (1994).
23. Schuchmann, K. & Müller, V. Energetics and Application of Heterotrophy in Acetogenic Bacteria. *Appl. Environ. Microbiol.* **82**, 4056–4069 (2016).
24. Abrini, J., Naveau, H. & Nyns, E.-J. Clostridium autoethanogenum, sp. nov., an anaerobic bacterium that produces ethanol from carbon monoxide. *Arch. Microbiol.* **161**, 345–351 (1994).
25. Foster, J. W., Foster, J. W. & Gillen, K. M. *Microbiology: An Evolving Science.* (W.W. Norton & Company, 2017).
26. Anukam, A., Mohammadi, A., Naqvi, M. & Granström, K. A Review of the Chemistry of Anaerobic Digestion: Methods of Accelerating and Optimizing Process Efficiency. *Processes* **7**, 504 (2019).
27. Ragsdale, S. W. & Pierce, E. Acetogenesis and the Wood-Ljungdahl Pathway of CO2 Fixation. *Biochim Biophys Acta* **1784**, 1873–1898 (2008).
28. Toerien, D. F. & Hattingh, W. H. J. Anaerobic digestion I. The microbiology of anaerobic digestion. *Water Research* **3**, 385–416 (1969).

29. Schink, B. Energetics of syntrophic cooperation in methanogenic degradation. *Microbiol Mol Biol Rev* **61**, 262–280 (1997).

30. Stams, A. J. M. Metabolic interactions between anaerobic bacteria in methanogenic environments. *Antonie van Leeuwenhoek* **66**, 271–294 (1994).

31. Wallrabenstein, C. & Schink, B. Evidence of reversed electron transport in syntrophic butyrate or benzoate oxidation by Syntrophomonas wolfei and Syntrophus buswellii. *Arch. Microbiol.* **162**, 136–142 (1994).

32. Plugge, C. M., Dijkema, C. & Stams, A. J. M. Acetyl-CoA cleavage pathway in a syntrophic propionate oxidizing bacterium growing on fumarate in the absence of methanogens. *FEMS Microbiology Letters* **110**, 71–76 (1993).

33. Baek, G., Kim, J., Kim, J. & Lee, C. Role and Potential of Direct Interspecies Electron Transfer in Anaerobic Digestion. *Energies* **11**, 107 (2018).

34. Aquino Neto, S., Reginatto, V. & De Andrade, A. R. Microbial Fuel Cells and Wastewater Treatment. in *Electrochemical Water and Wastewater Treatment* 305–331 (Elsevier, 2018). doi:10.1016/B978-0-12-813160-2.00012-2.

35. Stams, A. J. M. & Plugge, C. M. Electron transfer in syntrophic communities of anaerobic bacteria and archaea. *Nature Reviews Microbiology* **7**, 568–577 (2009).

36. Lindeboom, R. E. F., Fermoso, F. G., Weijma, J., Zagt, K. & van Lier, J. B. Autogenerative high pressure digestion: anaerobic digestion and biogas upgrading

in a single step reactor system. *Water Science and Technology* **64**, 647–653 (2011).

37. Lemmer, A., Merkle, W., Baer, K. & Graf, F. Effects of high-pressure anaerobic digestion up to 30 bar on pH-value, production kinetics and specific methane yield. *Energy* **138**, 659–667 (2017).
38. Kato, S. *et al.* The effects of elevated CO2 concentration on competitive interaction between aceticlastic and syntrophic methanogenesis in a model microbial consortium. *Front. Microbiol.* **5**, (2014).
39. Lindeboom, R. E. F., Shin, S. G., Weijma, J., van Lier, J. B. & Plugge, C. M. Piezo-tolerant natural gas-producing microbes under accumulating pCO2. *Biotechnology for Biofuels* **9**, (2016).
40. Anderson, K., Sallis, P. & Uyanik, S. Anaerobic treatment processes. in *Handbook of Water and Wastewater Microbiology* 391–426 (Elsevier, 2003). doi:10.1016/B978-012470100-7/50025-X.
41. Anstice, P. J. C. *et al.* Mechanistic study of on-line bicarbonate (hydrogencarbonate) monitoring of anaerobic sewage sludge digesters. *Analyst* **120**, 2873 (1995).
42. Murto, M., Björnsson, L. & Mattiasson, B. Impact of food industrial waste on anaerobic co-digestion of sewage sludge and pig manure. *Journal of*

Environmental Management **70**, 101–107 (2004).

43. Wang, Y., Zhang, Y., Wang, J. & Meng, L. Effects of volatile fatty acid concentrations on methane yield and methanogenic bacteria. *Biomass and Bioenergy* **33**, 848–853 (2009).
44. Franke-Whittle, I. H., Walter, A., Ebner, C. & Insam, H. Investigation into the effect of high concentrations of volatile fatty acids in anaerobic digestion on methanogenic communities. *Waste Manag* **34**, 2080–2089 (2014).
45. Jones, R. P. & Greenfield, P. F. Effect of carbon dioxide on yeast growth and fermentation. *Enzyme and Microbial Technology* **4**, 210–223 (1982).
46. Wan, R., Chen, Y., Zheng, X., Su, Y. & Huang, H. Effect of CO2 on NADH production of denitrifying microbes via inhibiting carbon source transport and its metabolism. *Science of The Total Environment* **627**, 896–904 (2018).
47. Lehninger, A. L., Nelson, D. L. & Cox, M. M. *Lehninger principles of biochemistry*. (W.H. Freeman, 2013).
48. Biebl, H., Menzel, K., Zeng, A.-P. & Deckwer, W.-D. Microbial production of 1,3-propanediol. *Applied Microbiology and Biotechnology* **52**, 289–297 (1999).
49. Clomburg, J. M. & Gonzalez, R. Anaerobic fermentation of glycerol: a platform for renewable fuels and chemicals. *Trends in biotechnology* **31**, 20–28 (2013).
50. Temudo, M. F., Poldermans, R., Kleerebezem, R. & van Loosdrecht, M. C. M.

Glycerol fermentation by (open) mixed cultures: A chemostat study. *Biotechnology and Bioengineering* **100**, 1088–1098 (2008).

51. María Paola Gómez Páez. Steering Product Formation in Anaerobic Digestion Systems: The effect of elevated CO2 partial pressure on the fermentative degradation of pyruvate and butyrate by a mixed microbial consortium. (Delft University of Technology, 2019).
52. Gonzalez-Garcia, R. *et al.* Microbial Propionic Acid Production. *Fermentation* **3**, 21 (2017).
53. Berg, I. A., Kockelkorn, D., Buckel, W. & Fuchs, G. A 3-hydroxypropionate/4-hydroxybutyrate autotrophic carbon dioxide assimilation pathway in Archaea. *Science* **318**, 1782–1786 (2007).
54. Merle de Kreuk, Nuria Marti, Yu Tao & Haoyu Wang. SMA Test. (2012).
55. Chafla, P. C. Protocol for setting up mixed culture fermentation at elevated CO2 experiments. (2018).
56. *Standard methods for the examination of water and wastewater*. (APHA, 1971).
57. Brown, M. R. *et al.* A flow cytometry method for bacterial quantification and biomass estimates in activated sludge. *Journal of Microbiological Methods* **160**, 73–83 (2019).
58. Magoc, T. & Salzberg, S. L. FLASH: fast length adjustment of short reads to

improve genome assemblies. *Bioinformatics* **27**, 2957–2963 (2011).

59. Bokulich, N. A. *et al.* Quality-filtering vastly improves diversity estimates from Illumina amplicon sequencing. *Nat Methods* **10**, 57–59 (2013).

60. Caporaso, J. G. *et al.* QIIME allows analysis of high-throughput community sequencing data. *Nat Methods* **7**, 335–336 (2010).

61. Edgar, R. C., Haas, B. J., Clemente, J. C., Quince, C. & Knight, R. UCHIME improves sensitivity and speed of chimera detection. *Bioinformatics* **27**, 2194–2200 (2011).

62. Edgar, R. C. UPARSE: highly accurate OTU sequences from microbial amplicon reads. *Nat Methods* **10**, 996–998 (2013).

63. Wang, Q., Garrity, G. M., Tiedje, J. M. & Cole, J. R. Naive Bayesian Classifier for Rapid Assignment of rRNA Sequences into the New Bacterial Taxonomy. *Applied and Environmental Microbiology* **73**, 5261–5267 (2007).

64. Quast, C. *et al.* The SILVA ribosomal RNA gene database project: improved data processing and web-based tools. *Nucleic Acids Research* **41**, D590–D596 (2012).

65. Edgar, R. C. MUSCLE: multiple sequence alignment with high accuracy and high throughput. *Nucleic Acids Research* **32**, 1792–1797 (2004).

66. Rittmann, B. E. & McCarty, P. L. *Environmental biotechnology: principles and applications*. (McGraw-Hill, 2007).

67. Heijnen, J. J. & Kleerebezem, R. Bioenergetics of Microbial Growth. in *Encyclopedia of Industrial Biotechnology* eib084 (John Wiley & Sons, Inc., 2010). doi:10.1002/9780470054581.eib084.

68. Miller, J. F., Shah, N. N., Nelson, C. M., Ludlow, J. M. & Clark, D. S. Pressure and Temperature Effects on Growth and Methane Production of the Extreme Thermophile Methanococcus jannaschii. *APPL. ENVIRON. MICROBIOL.* 4.

69. Zhuang, G.-C. *et al.* Effects of pressure, methane concentration, sulfate reduction activity, and temperature on methane production in surface sediments of the Gulf of Mexico. *Limnology and Oceanography* **63**, 2080–2092 (2018).

70. Fast, A. G. & Papoutsakis, E. T. Stoichiometric and energetic analyses of non-photosynthetic CO2-fixation pathways to support synthetic biology strategies for production of fuels and chemicals. *Current Opinion in Chemical Engineering* **1**, 380–395 (2012).

71. Li, W.-J. *et al.* Georgenia ruanii sp. nov., a novel actinobacterium isolated from forest soil in Yunnan (China), and emended description of the genus Georgenia. *INTERNATIONAL JOURNAL OF SYSTEMATIC AND EVOLUTIONARY MICROBIOLOGY* **57**, 1424–1428 (2007).

72. Wang, S., Xu, X., Wang, L., Jiao, K. & Zhang, G. Georgenia subflava sp. nov., isolated from a deep-sea sediment. *International Journal of Systematic and*

Evolutionary Microbiology, **65**, 4146–4150 (2015).

73. Kerfahi, D. *et al.* Shallow Water Marine Sediment Bacterial Community Shifts Along a Natural CO2 Gradient in the Mediterranean Sea Off Vulcano, Italy. *Microb Ecol* **67**, 819–828 (2014).
74. Wang, Z., Sun, J., Zhang, A. & Yang, S.-T. Propionic Acid Fermentation. in *Bioprocessing Technologies in Biorefinery for Sustainable Production of Fuels, Chemicals, and Polymers* (eds. Yang, S.-T., El-Enshasy, H. A. & Thongchul, N.) 331–350 (John Wiley & Sons, Inc., 2013). doi:10.1002/9781118642047.ch18.
75. Howard, D. H. THE PRESERVATION OF BACTERIA BY FREEZING IN GLYCEROL BROTH, 12. *J Bacteriol* **71**, 625 (1956).
76. Worm, P. *et al.* A genomic view on syntrophic versus non-syntrophic lifestyle in anaerobic fatty acid degrading communities. *Biochimica et Biophysica Acta (BBA) - Bioenergetics* **1837**, 2004–2016 (2014).
77. Yu, T. & Chen, Y. Effects of elevated carbon dioxide on environmental microbes and its mechanisms: A review. *Science of The Total Environment* **655**, 865–879 (2019).
78. Liu, Y., Balkwill, D. L., Aldrich, H. C., Drake, G. R. & Boone, D. R. Characterization of the anaerobic propionate-degrading syntrophs Smithella propionica gen. nov., sp. nov. and Syntrophobacter wolinii. *Int. J. Syst. Bacteriol.*

49 Pt 2, 545–556 (1999).

79. de Bok, F. A., Stams, A. J., Dijkema, C. & Boone, D. R. Pathway of propionate oxidation by a syntrophic culture of Smithella propionica and Methanospirillum hungatei. *Appl. Environ. Microbiol.* **67**, 1800–1804 (2001).

80. Fang, H. H. P., Chui, H.-K. & Li, Y.-Y. Anaerobic degradation of butyrate in a UASB reactor. *Bioresource Technology* **51**, 75–81 (1995).

Appendix

Appendix A. Inoculation principles

There are two principles for inoculation; one is Gas: Liquid ratio, and the other is Substrate: Inoculum ratio.[55]

Principle 1: Gas and liquid distribution

Gas: liquid ratio of 1:1.5 has shown to be a safe choice from previous experiments. With the consideration of the physical and chemical properties of biogas production, the system pressure increases when the anaerobic digestion is fully completed to the final step. Therefore, the selection estimated the methane production where the headspace provides enough range to sustain the pressure increment.

Principle 2: Substrate-to-inoculum ratio (S/I)

The chosen S/I ratio is 0.5. S/I ratio is an essential parameter affecting the performance of the anaerobic digestion process; an inappropriate S/I ratio could cause inhibition to production or degradation. To keep the consistency of the experiments, the inoculation volumes were estimated according to the following equations (Eq. A1 and Eq. A2)

$$V_{sub} + V_{sludge} = V_{liquid} \quad \text{(Eq. A. 1)}$$

$$\frac{V_{sub} * COD_{sub}}{V_{sludge} * VSS_{sludge}} = 0.5 \quad \text{(Eq. A. 2)}$$

Appendix B. Theoretical calculations for culture enrichment

Inoculation			
V_bottle	2000	I:S	0.499759
Liquid	1200	V_sub	1041.753
Gas	800	V_slu	158.2472

Actual yield from 0th cycle							
	Filter	First	Second	TSS	VSS	AVG	Yield
Gly-1	2.4834	2.5075	2.4879	2.41	1.96	1.915	0.21
Gly-2	2.5061	2.5296	2.5109	2.35	1.87		
Glu-1	2.5187	2.5696	2.53	2.545	1.98	1.9975	0.30
Glu-2	2.5023	2.5555	2.5152	2.66	2.015		

Enrichment			
Stock solution	3.60 g COD/L	Glucose	3.71 g/L
		Glycerol	2.99 g/L
Sludge conc.	13.17 g VSS/L	Theo. Y	0.06 g VSS/g COD
Inoculum conc.	1.74 g VSS/L	Glu. Y	0.21 g VSS/g COD
Withdral volume	240.00 ml	Gly. Y	0.30 g VSS/g COD

Theoretical Yield			
cycle	VSS		S:I
0th cycle	1.44	g/L	0.50
1st cycle	1.21	g/L	0.60
2nd cycle	1.02	g/L	0.71
3rd cycle	0.86	g/L	0.83
4th cycle	0.74	g/L	0.97
5th cycle	0.65	g/L	1.11
Obtained biomass	0.78	g	

Glucose Yield			
cycle	VSS		S:I
0th cycle	1.57	g/L	0.46
1st cycle	1.43	g/L	0.50
2nd cycle	1.32	g/L	0.54
3rd cycle	1.24	g/L	0.58
4th cycle	1.17	g/L	0.62
5th cycle	1.11	g/L	0.65
Obtained biomass	1.33	g	

Glycerol Yield			
cycle	VSS		S:I
0th cycle	1.65	g/L	0.44
1st cycle	1.58	g/L	0.46
2nd cycle	1.52	g/L	0.47
3rd cycle	1.48	g/L	0.49
4th cycle	1.44	g/L	0.50
5th cycle	1.41	g/L	0.51
Obtained biomass	1.70	g	

Appendix C. Overall stoichiometry

According to the end-product spectrums, the overall fermentation stoichiometries can be generated.

U0.3: $0.042C_6H_{12}O_6 + 0.25H_2O \rightarrow 0.125CH_4 + 0.375CO_2$
U1: $0.042C_6H_{12}O_6 + 0.25H_2O \rightarrow 0.125CH_4 + 0.375CO_2$
U3: $0.042C_6H_{12}O_6 + 0.092H_2O + 0.032HCO_3^- \rightarrow 0.071CH_4 + 0.26CO_2 + 0.002C_2H_3O_2^- + 0.030C_3H_5O_2^-$
U5: $0.042C_6H_{12}O_6 + 0.054H_2O + 0.002HCO_3^- \rightarrow 0.056CH_4 + 0.228CO_2 + 0.039C_3H_5O_2^-$
U8: $0.042C_6H_{12}O_6 + 0.055H_2O + 0.039HCO_3^- \rightarrow 0.058CH_4 + 0.26CO_2 + 0.002C_4H_7O_2^- + 0.037C_3H_5O_2^-$
$U5E$: $0.042C_6H_{12}O_6 + 0.146H_2O + 0.018HCO_3^- + 0.008NH_4^+ \rightarrow 0.094CH_4 + 0.301CO_2 + 0.009C_2H_3O_2^- + 0.002C_3H_5O_2^- + 0.008C_2H_5O_2N$
$Y0.3$: $0.071C_3H_8O_3 + 0.165H_2O + 0.006NH_4^+ + 0.006HCO_3^- \rightarrow 0.111CH_4 + 0.304CO_2 + 0.006C_2H_5O_2N$
$Y1$: $0.071C_3H_8O_3 + 0.041H_2O + 0.008NH_4^+ + 0.033HCO_3^- \rightarrow 0.071CH_4 + 0.215CO_2 + 0.011C_2H_3O_2^- + 0.014C_3H_5O_2^- + 0.008C_2H_5O_2N$
$Y3$: $0.071C_3H_8O_3 + 0.008NH_4^+ + 0.051HCO_3^- \rightarrow 0.030CH_4 + 0.127CO_2 + 0.001C_2H_3O_2^- + 0.042C_3H_5O_2^- + 0.010C_2H_5O_2N + 0.072H_2O$
$Y5$: $0.071C_3H_8O_3 + 0.010NH_4^+ + 0.053HCO_3^- \rightarrow 0.025CH_4 + 0.114CO_2 + 0.001C_2H_3O_2^- + 0.042C_3H_5O_2^- + +0.001C_4H_7O_2^- + 0.010C_2H_5O_2N + 0.089H_2O$
$Y8$: $0.071C_3H_8O_3 + 0.022NH_4^+ + 0.043HCO_3^- \rightarrow 0.034CH_4 + 0.118CO_2 + 0.002C_2H_3O_2^- + 0.016C_3H_5O_2^- + +0.002C_4H_7O_2^- + 0.022C_2H_5O_2N + 0.087H_2O$
$Y5E$: $0.071C_3H_8O_3 + 0.139H_2O + 0.015HCO_3^- \rightarrow 0.099CH_4 + 0.283CO_2 + 0.015C_3H_5O_2^-$